Journal of Applied Fluid Mechanics, Vol. 18, No. 1, pp. 241-259, 2025.
Available online at www.jafmonline.net, ISSN 1735-3572, EISSN 1735-3645.
https://doi.org/10.47176/jafm.18.1.2427

Longitudinal Sloshing Behaviors of Horizontal Cylindrical Liquid Tanks Subjected to Harmonic and Seismic Excitations

A. H. Daneshmand [1], A. Karamodin [2†] and M. Pasandideh Fard [3]

[1] *Department of Civil Engineering, Ferdowsi University of Mashhad, Mashhad, Iran*
[2] *Department of Civil Engineering, Faculty of Engineering, Ferdowsi University of Mashhad, Mashhad, Iran*
[3] *Department of Mechanical Engineering, Faculty of Engineering, Ferdowsi University of Mashhad, Mashhad, Iran*

†*Corresponding author Email: a-karam@um.ac.ir*

ABSTRACT

In the present study, the sloshing behavior of horizontal cylindrical liquid tanks under longitudinal excitation is investigated numerically. Shallow liquid wave theory has been used to derive the equations governing fluid motion. In the numerical model, the effect of shear stress on the bottom of the horizontal cylindrical tank is considered by solution of the Navier – Stokes equations in the longitudinal direction. Numerical results have been validated by approximating the cross-sectional area of a liquid-filled segment to a rectangular cross-section using available numerical and experimental studies on a rectangular tank, which a good conformity is observed. The sloshing behavior of horizontal cylindrical tank fluid has been compared with rectangular tank fluid in terms of maximum wave elevation and force applied to the tank's lateral wall, under harmonic and seismic excitations. The results show that the force applied to the lateral wall of the cylindrical tank is higher than that of the rectangular tank, in some cases. In addition, the horizontal cylindrical tank can be used as an alternative of the rectangular tank with almost the same volume of water but 26 % less length on average. Finally, the effect of viscosity and density of fluid to the force created on the lateral wall of the horizontal cylindrical tank is investigated. It has been shown that the effect is negligible, so that if the viscosity of the fluid is greatly increased, the horizontal force applied to the tank's lateral wall decreases slightly.

Article History

Received November 13, 2023
Revised July 21, 2024
Accepted July 24, 2024
Available online November 6, 2024

Keywords:

Longitudinal liquid sloshing
Seismic excitation
Horizontal cylindrical tank
Shallow liquid wave theory
Shear stress of liquid tank bottom

1. INTRODUCTION

The presence of a free surface in tanks partially filled with a liquid causes the fluid to move in relation to the tank, and the phenomenon of liquid sloshing occurs under external excitations. Liquid sloshing inside the tank caused by external excitation is important to safety and engineering applications, including storage tanks for various fluids (water, oil, and chemicals), and energy loss in satellites (Bhuta & Koval, 1966), marine vessels (Carrier & Miles, 1960), and structure control by liquid dampers (Shimizu & Hayama, 1987). Damage to these tanks can lead to adverse effects such as water shortage, fire, environmental pollution, and consequent economic and social losses. Therefore, these critical tanks must perform satisfactorily against excitation caused by strong winds and earthquakes. Predicting the maximum sloshing wave elevation and the resulting force applied to the tank's lateral wall are the main considerations in the seismic design and engineering applications of liquid containers.

Solving liquid sloshing equations depends strongly on the shape of the tank. Practically, most liquid storage tanks are rectangular or cylindrical, and the fluid depth can be deep or shallow, depending on the purpose and application. Numerous analytical, numerical, and experimental studies have investigated sloshing in partially filled tanks. Analytical solutions based on linear wave theory are useful for evaluating low-amplitude fluid motion. Housner (1963) first proposed an analytical spring-mass model for liquid sloshing in tanks using linear wave theory. Chen and Chiang (2000) analyzed the sloshing flow inside a floating tank using the Euler equation. Wu et al. (2001) proposed an analytical solution based on Navier – Stokes linear equations to investigate sloshing waves inside a rectangular tank. The use of linear wave theory under severe excitation does not show the actual behavior of the sloshing liquid. Therefore,

numerous studies have been performed over the past three decades on the nonlinear behavior of sloshing waves to predict maximum forces due to liquid sloshing under large excitations such as earthquakes. Koh et al. (1994) proposed a theoretical model for the study of shallow fluid motion in a rectangular tank under arbitrary horizontal excitation. Chen et al. (1996) used the finite difference method to simulate the nonlinear motion of liquid sloshing in a rectangular tank under seismic excitation. Frandsen (2004) developed a nonlinear model to study the liquid sloshing phenomenon in a tank that can move in both horizontal and vertical directions. Lu et al. (2004) proposed a new numerical model to simulate fluid sloshing in a rectangular tank under a pair of horizontal and rotational motions. In Lu's model, the shallow liquid wave theory is continuously used to derive the motion equations so that this model can be used for huge sloshing including hydraulic jump. Chen et al. (2007) presented a numerical model based on the boundary element method and the expansion of the second Taylor series to study the sloshing behavior of rectangular and vertical cylindrical liquid tanks. In their study, the height and force of the sloshing wave inside the liquid tanks under harmonic and seismic excitations were evaluated. Virella et al. (2008) investigated the natural period of sloshing, shape modes, and modal pressure distributions by applying linear and nonlinear wave theory. Ibrahim (2005), and Faltinsen and Timokha (2009) published comprehensive reviews on linear and nonlinear analytical modeling under different sloshing excitation conditions such as swaying and rolling. Goudarzi and Sabbagh-Yazdi (2012) and Hejazi and Mohammadi (2019) performed a series of shaking table experiments to investigate the nonlinear behavior of liquid sloshing inside rectangular tanks under harmonic motions by various earthquakes and compared them with nonlinear numerical results; the performed experiments were well consistent with nonlinear numerical results. Recently, nonlinear sloshing analyses have been performed on rectangular tanks (Moslemi et al., 2019; Yan et al., 2020; Gao et al., 2021), tanks with a sloped bottom (Pandit & Biswal, 2020), tanks with a sloped wall (Roy & Biswal, 2023) and tanks with arbitrary shapes (Gholamipoor & Ghiasi, 2022).

Most studies on horizontal cylindrical tanks have focused on semi-analytical, numerical or experimental calculation of sloshing frequency in these tanks (Moiseev & Petrov, 1966; McIver & McIver, 1993; Gurusamy & Kumar, 2020, 2021). A number of other studies on horizontal cylindrical tanks have been limited to the specific half-full case of these tanks (Evans & Linton, 1993; Papaspyrou et al., 2004; Karamanos & Kouka, 2016; Saghi & Saghi, 2022). Timokha (2007) developed an approximate formula for calculating the natural longitudinal sloshing frequencies of shallow fluid in horizontal cylindrical tanks using the Rayleigh quotient. The results showed that the proposed formula, with a number of dimensional constraints in accordance with the Shallow liquid wave theory, has good accuracy for the first sloshing mode and is useful for engineering applications. Kobayashi et al. (1989) experimentally studied the natural frequencies and liquid sloshing forces in horizontal cylindrical tanks in both longitudinal and transverse directions and compared the results with the equivalent rectangular tank. Dai and Xu (2006) proposed a numerical approach on the analysis of sloshing liquids in horizontal cylindrical tanks; in the introduced method, potential flow theory is used and the study is performed on the half-full of the tank. Using potential flow theory, Patkas and Karamanos (2007) developed a semi-analytical mathematical model to calculate the effects of linear sloshing on the dynamic response of horizontal and spherical cylindrical tanks under external excitation; the results showed that by increasing the liquid depth, the mass of the liquid participating in the sloshing is decreased.

Nonetheless, few studies have investigated the nonlinear behavior of shallow liquid sloshing during longitudinal excitation of horizontal cylindrical tanks. Shallow liquid horizontal cylindrical tanks have a wide range of applications in engineering as energy dissipation systems (e.g., as damper in the seismic control of structures) because of the large mass participation of the liquid in sloshing during the longitudinal excitation of the tank. As far as the current authors know, shallow liquid wave theory has not yet been used for the longitudinal sloshing analysis of fluid in shallow horizontal cylindrical tanks. Therefore, this study, inspired by the Lu et al. (2004) model, has focused on the numerical investigation of shallow liquid sloshing inside a horizontal cylindrical tank under longitudinal excitation, with continuous use of shallow liquid wave theory in one-dimensional assumption. Hence, at first, the equations governing shallow liquid sloshing inside the horizontal cylindrical tank were extracted. Then, to consider the effects of the tank bottom, the Navier – Stokes equations were solved in polar coordinates and in the longitudinal direction of the tank to obtain the relationship between the shear stress at the bottom of the tank and the fluid velocity. To calculate the fluid sloshing frequency and design horizontal cylindrical tanks under longitudinal excitation, the approximate relationship proposed by Timokha (2007) was used, which is suitable for shallow liquid wave theory. The maximum wave elevation and sloshing force of the fluid applied to the lateral wall of the tanks were calculated under harmonic and seismic excitations. Then the results were compared with those of rectangular tanks studied experimentally and numerically by Chen et al. (2007), and theoretically by Lu et al. (2004). Finally, a brief study of the force difference created on the lateral wall of the horizontal cylindrical tank resulting from the sloshing of fluids with different viscosities and densities has been performed. In fact, in this research, an attempt has been made to determine the differences between the selection of rectangular tanks and horizontal cylinders and their fluid type for engineering purposes in a practical and simple manner.

2. NUMERICAL MODEL

2.1. Governing Equations

The rigid horizontal cylindrical tank shown in Fig. 1, is considered for this study. The length and radius of the tank, and initial depth of the liquid are denoted by L_c, R and h_0, respectively. H and L represent the maximum

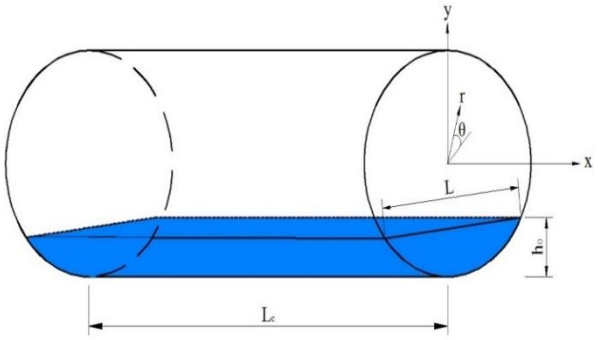

(a)

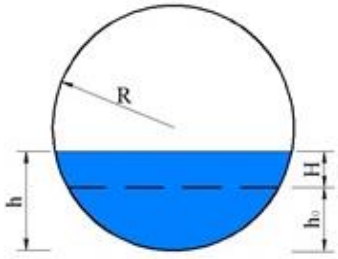

(b)

Fig. 1 Schematic of the rigid horizontal cylindrical tank at (a) steady state and (b) side view in sloshing with maximum depth h

wave elevation formed relative to the initial depth of the liquid and the length of the liquid free surface inside the tank, respectively.

The shallow liquid wave theory was utilized to model the sloshing motion of the liquid inside the tank under horizontal excitation. In this theory, it is assumed that the vertical component of liquid particle acceleration has little effect on the liquid pressure; thus, the liquid pressure is considered hydrostatic. Moreover, the velocity profile is considered uniform in the vertical cross section (Stoker, 2011). With this theory, the governing equations were derived using the two principles of mass and momentum continuity (Stoker, 2011), and details of their extraction are given in Appendix A. As a result, the equations governing liquid sloshing inside the horizontal cylindrical tank along the length of the tank which have been achieved are given as:

$$V\left(\frac{4Rh-2h^2}{\sqrt{2Rh-h^2}}\right)\frac{\partial h}{\partial x}+\left(R^2\cos^{-1}\left(\frac{R-h}{R}\right)-(R-h)\sqrt{2Rh-h^2}\right)\frac{\partial V}{\partial x} \quad (1)$$
$$+\left(\frac{4Rh-2h^2}{\sqrt{2Rh-h^2}}\right)\frac{\partial h}{\partial t}=0$$

$$\frac{\partial V}{\partial t}+V\frac{\partial V}{\partial x}+g\frac{\partial h}{\partial x}+gS+\frac{\partial^2 x_B}{\partial t^2}=0 \quad (2)$$

with boundary conditions:

$$V\big|_{x=0}=V\big|_{x=Lc}=0 \quad (3)$$

and initial conditions:

$$h\big|_{t=0}=h_0 \text{ and } V\big|_{t=0}=0 \quad \forall x\in[0,L_c] \quad (4)$$

In the above equations, g is the gravitational acceleration, V is the longitudinal velocity of the liquid relative to the bottom of the tank, and h is the maximum depth of sloshing flow at location x (longitudinal direction of the tank) and moment t. The term $\frac{\partial^2 x_B}{\partial t^2}$ indicates the acceleration applied to the tank in the longitudinal direction. In addition, S is the slope of the energy grade lines (Henderson, 1966), which is related to the shear stress at the bottom of the tank (τ) by the following equation:

$$S=\frac{\tau}{\rho g\left(\frac{R}{2}-\frac{(R-h)L}{4R\cos^{-1}\left(\frac{R-h}{R}\right)}\right)} \quad (5)$$

where ρ is the fluid density. Appendix A describes how to obtain the slope of the energy grade lines (Eq. 5) for a horizontal cylindrical tank with a circular cross section.

The approximate relation of the maximum shear stress at the horizontal cylindrical tank bottom is presented here for viscous fluid in one dimension (calculation details for this equation are presented in Appendix B):

$$\tau=\sqrt{2}\frac{D}{C_1}\rho\sqrt{\omega\vartheta}V_{max} \quad (6)$$

where ω and ϑ represent the circular frequency of the vibration and the kinetic viscosity of the fluid, respectively. The relations of the two coefficients D and C_1 are presented in Appendix B. V_{max} indicates the maximum fluid velocity relative to the tank. In the shallow liquid wave theory, the velocity distribution is uniform at the vertical cross-section of the flow; for simplification, the velocity obtained from solving the governing Eqs. (1) and (2) was considered the average velocity (V_{avg}) of the cross-section. According to Koh et al. (1994), given the shallow liquid depth, it is reasonable to replace V_{max} with V_{avg}. The result of Eq. (6) is as follows:

$$\tau=\sqrt{2}\frac{D}{C_1}\rho\sqrt{\omega\vartheta}V_{avg} \quad (7)$$

Note that if the liquid depth is very shallow (less than 1 cm), the presence of a boundary layer at the tank bottom makes it necessary to adjust the relationship between the average and maximum velocities (Lu et al., 2004).

Although both mass and momentum continuity principles are generally applicable regardless of the amount of liquid sloshing inside the tank, it is necessary to limit the ratio of the maximum initial liquid depth to the tank radius ($\frac{h_0}{R}$), to ensure that the liquid does not collide with the top of the tank during sloshing. According to coastal engineering, when the water depth is shallow, the wave break, depending on the beach slope and the type of break, occurs when $0.4<\frac{H}{h_0}<1.2$ (Reeve et al., 2018). Therefore, considering the worst case (i.e., wave break

occurs at $\frac{H}{h_0}=1.2$), the $\frac{h_0}{R}$ ratio can be selected as a maximum of 0.9. In this case, the maximum sloshing wave elevation will break at a maximum elevation of 1.98*R* before hitting the top of the tank (2*R*):

$$\frac{h_0}{R}=0.9\rightarrow h_0=0.9R\rightarrow$$
$$h_{max}=0.9R+\left(1.2\times 0.9R\right)=1.98R \tag{8}$$

According to the assumption of hydrostatic pressure in shallow liquid wave theory, the sloshing force applied to the tank's lateral wall is obtained from the following equations:

if $h<R$:

$$F=\rho g\left(h_R-\left(R-\frac{4R\left(\frac{L_R}{2R}\right)^3}{3\left(2\cos^{-1}\left(\frac{R-h_R}{R}\right)-\frac{(R-h_R)L_R}{R^2}\right)}\right)\right)\left(R^2\cos^{-1}\left(\frac{R-h_R}{R}\right)-\frac{(R-h_R)L_R}{2}\right)$$
$$-\rho g\left(h_L-\left(R-\frac{4R\left(\frac{L_L}{2R}\right)^3}{3\left(2\cos^{-1}\left(\frac{R-h_L}{R}\right)-\frac{(R-h_L)L_L}{R^2}\right)}\right)\right)\left(R^2\cos^{-1}\left(\frac{R-h_L}{R}\right)-\frac{(R-h_L)L_L}{2}\right) \tag{9}$$

and if $h>R$:

$$F=\rho g\left(\pi R^3-\left(\left(2R-\frac{4R\left(\frac{L_R}{2R}\right)^3}{3\left(2\cos^{-1}\left(\frac{h_R-R}{R}\right)-\frac{(h_R-R)L_R}{R^2}\right)}\right)\left(R^2\cos^{-1}\left(\frac{h_R-R}{R}\right)-\frac{(h_R-R)L_R}{2}\right)\right)\right)$$
$$-\rho g\left(\pi R^3-\left(\left(2R-\frac{4R\left(\frac{L_L}{2R}\right)^3}{3\left(2\cos^{-1}\left(\frac{h_L-R}{R}\right)-\frac{(h_L-R)L_L}{R^2}\right)}\right)\left(R^2\cos^{-1}\left(\frac{h_L-R}{R}\right)-\frac{(h_L-R)L_L}{2}\right)\right)\right) \tag{10}$$

h_R and L_R represent the maximum height and length of the liquid free surface in the right lateral wall of the tank, respectively; and h_L and L_L represent the maximum height and length of the liquid free surface in the left lateral wall of the tank, respectively.

2.2. Solution Procedure

In this study, the equations governing water sloshing inside a horizontal cylindrical tank were solved numerically using the Lax Finite Difference Scheme (Lu et al., 2004). In the first time step, the governing Eqs. (1) and (2) were solved with the appropriate boundary and initial conditions (Eqs. 3 and 4). As a result, the maximum water height on both sides of the tank (h_R and h_L) was obtained for the next time step, plus the sloshing force F (using Eq. 9 or 10). These calculations were repeated until the final time step. The variables of Eqs. (1) and (2) can be calculated according to the Lax Finite Difference Scheme as follows (Lu et al., 2004):

$$\frac{\partial \hat{f}}{\partial t}=\frac{\hat{f}_j^{(k+1)}-\left[\phi\hat{f}_j^{(k)}+\frac{(1-\phi)(\hat{f}_{j+1}^{(k)}+\hat{f}_{j-1}^{(k)})}{2}\right]}{\Delta t} \tag{11}$$

$$\hat{f}=\phi\hat{f}_j^{(k)}+\frac{(1-\phi)(\hat{f}_{j+1}^{(k)}+\hat{f}_{j-1}^{(k)})}{2} \tag{12}$$

$$\frac{\partial \hat{f}}{\partial x}=\frac{\hat{f}_{j+1}^{(k)}-\hat{f}_{j-1}^{(k)}}{2\Delta x} \tag{13}$$

In the above relations, $\hat{f}$ is a general variable that can represent any of the variables *h*, *V* or *S*. Also, the *k* superscript represents the moment in time $k\Delta t$, where Δt is the time step. The j subscript represents the node at the location $j\Delta x$ along the tank (L_c), where Δx is the element length. The ϕ parameter can have a value between 0 and 1. The value of ϕ in this study is considered to be 0.98. Further details on the effect of the ϕ parameter are discussed by Lu et al. (2004).

The value of Δx in Eq. (13) is obtained by dividing the tank length to appropriate number of divisions (*n*). The minimum value of n is calculated from the following equation (Shimizu & Hayama, 1987):

$$n=\frac{\pi}{2\arccos\left(\sqrt{\frac{\tanh(\pi\varepsilon)}{2\tanh\left(\frac{\pi\varepsilon}{2}\right)}}\right)}\quad,\quad \varepsilon=\frac{h_0}{\left(\frac{L_c}{2}\right)} \tag{14}$$

Furthermore, for a stable numerical solution, the maximum value of Δt is limited to the following relation (Lu et al., 2004):

$$\Delta t\le\frac{\Delta x}{max\left(|V|+\sqrt{gh}\right)} \tag{15}$$

In this research, a time step of 0.001 seconds was used to satisfy the above relation.

2.3. Horizontal Cylindrical Tank Design Considerations

Timokha has presented an approximate analytical relation for calculating the natural frequency of longitudinal sloshing of incompressible fluid in a horizontal cylindrical tank (Timokha, 2007). The approximate Timokha relation for the first mode of longitudinal sloshing of liquid is as follows (Timokha, 2007):

$$\omega_c=\frac{\pi R}{L_c}\sqrt{\frac{g}{R}\,\mathrm{W}\left(\frac{h_0}{R}\right)} \tag{16}$$

where $\mathcal{W}$ is:

$$\mathrm{W}\left(\frac{h_0}{R}\right)=\frac{F\left(\frac{h_0}{R}\right)}{2a\left(\frac{h_0}{R}\right)} \tag{17}$$

Table 1 Permitted ranges of the $\frac{h_0}{R}$ ratio

$\frac{h_0}{L_c}$	Permitted ranges of the $\frac{h_0}{R}$
$\frac{h_0}{L_c}=0.15$	$0.75 \le \frac{h_0}{R} \le 0.9$
$\frac{h_0}{L_c}=0.125$	$0.625 \le \frac{h_0}{R} \le 0.9$
$\frac{h_0}{L_c}=0.10$	$0.50 \le \frac{h_0}{R} \le 0.9$
$\frac{h_0}{L_c}=0.075$	$0.375 \le \frac{h_0}{R} \le 0.9$
$\frac{h_0}{L_c}=0.05$	$0.25 \le \frac{h_0}{R} \le 0.9$

$$\mathrm{F}\left(\frac{h_0}{R}\right)=\begin{cases} arctan\left(\dfrac{\alpha\left(\frac{h_0}{R}\right)}{\beta\left(\frac{h_0}{R}\right)}\right)-\alpha\left(\frac{h_0}{R}\right)\beta\left(\frac{h_0}{R}\right), & 0\le\frac{h_0}{R}\le 1 \\ \pi+arctan\left(\dfrac{\alpha\left(\frac{h_0}{R}\right)}{\beta\left(\frac{h_0}{R}\right)}\right)-\alpha\left(\frac{h_0}{R}\right)\beta\left(\frac{h_0}{R}\right), & 1\le\frac{h_0}{R}\le 2 \end{cases} \tag{18}$$

$$\alpha\left(\frac{h_0}{R}\right)=\sqrt{1-\left(1-\frac{h_0}{R}\right)^2} \tag{19}$$

$$\beta\left(\frac{h_0}{R}\right)=1-\frac{h_0}{R} \tag{20}$$

Timokha's analysis of the comparison between the experimental results and Eq. (16) shows that this equation can be used to calculate the first mode of longitudinal sloshing frequency of a shallow liquid inside a horizontal cylinder tank with an error of less than 5%, provided that the following restrictions are observed (Timokha, 2007):

$$\frac{L_c}{R}\ge 5 \quad \text{And} \quad \frac{h_0}{R}\le 1.6 \tag{21}$$

Previously, the maximum allowable value of $\frac{h_0}{R}$ was limited to 0.9 to prevent the liquid from hitting the top of the tank according to Eq. (8). On the other hand, the $\frac{h_0}{L_c}\le 0.15$ restriction in Shallow liquid wave theory and the $\frac{L_c}{R}\ge 5$ restriction in Eq. (21), lead to a minimum limit for the $\frac{h_0}{R}$ ratio. Due to the mentioned limitations, Table 1 presents the permitted ranges of the $\frac{h_0}{R}$ ratio for several different ratios of $\frac{h_0}{L_c}$.

3. RESULTS AND DISCUSSION

In this section, several examples are provided for review and discussion. First, the shear stress relationship of the horizontal cylindrical tank bottom (Eq. 7) and other relationships and the solution process presented in Section 2, have been validated using the relationships and results of the rectangular tank. Then, the maximum height of the fluid and the resulting force on the lateral wall of the horizontal cylindrical tank under the harmonic and seismic excitations of Kobe and Chi-Chi earthquakes are investigated in different conditions and the results are compared with a rectangular tank. Finally, the effect of different fluids with different dynamic viscosities and densities on the force applied to the lateral wall of the horizontal cylindrical tank during sloshing is investigated.

3.1. Validation of Shear Stress Relationship

Koh et al. (1994) and Lu et al. (2004) presented the shear stress relationship of the rectangular tank bottom under excitation for shallow fluid depths in the longitudinal direction as follows:

$$\tau=\rho\sqrt{\vartheta\omega}V_{avg} \tag{22}$$

The comparison of Eqs. (7) and (22) showed that the difference between the shear stress of the horizontal cylindrical and rectangular tank bottom is in the $f=\frac{\sqrt{2}D}{C_1}$ coefficient. In Figs. 2(a) and 2(b), the f coefficient in terms of radius for a horizontal cylindrical tank with h_0 = 0.7 cm and ω = 2 rad/s and a horizontal cylindrical tank with h_0 = 0.07 cm and ω = 0.02 rad/s are plotted, respectively.

As shown in Fig. 2, for both tanks with different initial water depths and frequencies, the coefficient f is not dependent on the radius but tended towards one. As a result, due to the one-dimensionality of the study, the shear stress formula for horizontal cylindrical tank bottom (Eq. 7) is with 1-3% deviation from that of rectangular tank bottom (Eq. 22). This indicates the accuracy of the relationship obtained for the shear stress of the horizontal cylindrical tank bottom (Eq. 7).

3.2. Comparison of Water Sloshing Behavior

In this section, the time history diagrams of maximum water height and force on the lateral wall of a horizontal cylindrical tank are compared with a rectangular tank with the same initial depth and length. The time history diagrams of maximum water height and force on the lateral wall of a rectangular tank are plotted by solving the equations presented by Lu et al. (2004) based on Shallow liquid wave theory, using the finite difference method.

The sloshing frequency of the fluid inside the rectangular tank is calculated according to the following formula (Stoker, 2011):

$$\omega_R=\sqrt{\frac{\pi g}{L_{re}}tanh\left(\frac{\pi h_0}{L_{re}}\right)} \tag{23}$$

where L_{re} stands for rectangular tank length. In this study, the rectangular tank frequency is considered 0.5 rad/s and $\frac{h_0}{L_{re}}=0.05$. As a result, according to Eq. (23), the length of the rectangular tank is 19.19 m, and the initial water

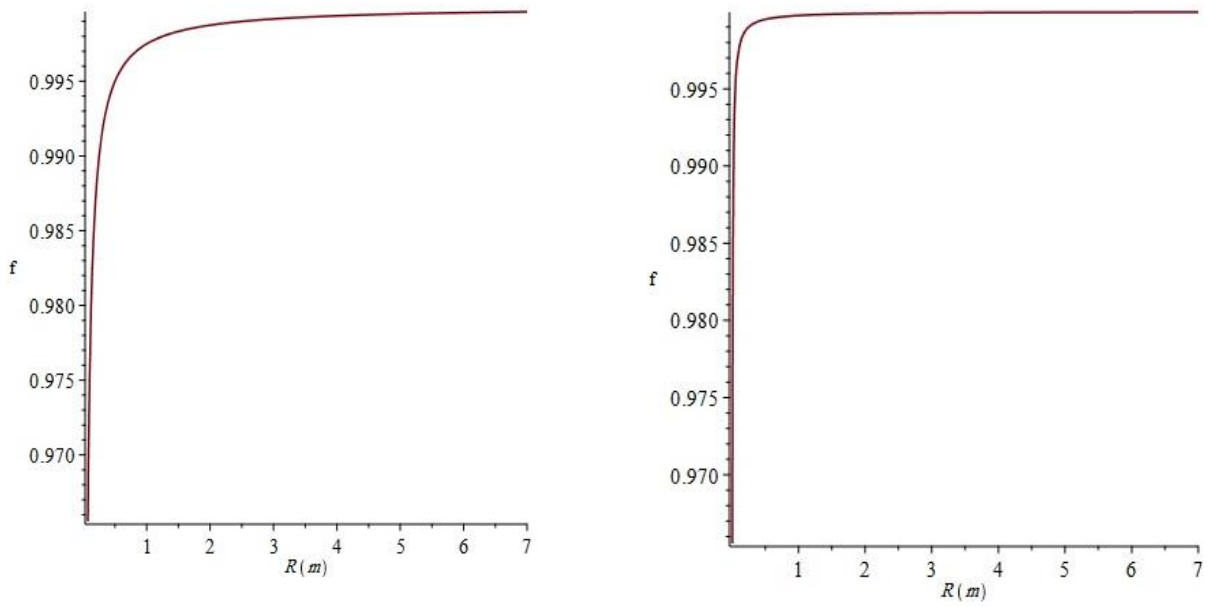

(a) (b)

Fig. 2 Coefficient f versus radius (R) (a) $\omega = 2$ rad/s, $h_0 = 0.7$ cm (b) $\omega = 0.02$ rad/s, $h_0 = 0.07$ cm

depth is 0.96 m. The initial depth and length of water inside the horizontal cylindrical tank is considered similar to the rectangular tank. The mesh size n = 160 is applied to satisfy the conditions of Eq. (14). Clearly, the higher the $\frac{h_0}{R}$ ratio is, the closer the segmental area of the circle filled with water is to the area of the rectangle. According to Table 1, the permitted range for the $\frac{h_0}{R}$ ratio for the horizontal cylindrical tank is between 0.25 and 0.9. Considering $\frac{h_0}{R} = 0.9$ for the horizontal cylindrical tank, the radius, frequency, and free surface length of fluid (L) are equal to 1.067 m, 0.44 rad/s, and 2.1232 m, respectively; considering $\frac{h_0}{R} = 0.9$, the radius, frequency, and free surface length of fluid (L) are 3.84 m, 0.415 rad/s, and 5.0798 m, respectively. As can be seen, the frequencies of the cylindrical and rectangular tanks are close to each other. Therefore, in Fig. 3, the time history diagrams of the force on the lateral wall of horizontal cylindrical tanks with $\frac{h_0}{R} = 0.9$ and $\frac{h_0}{R} = 0.25$ are compared with the force on the lateral wall of rectangular tanks with widths of 2.1232 m and 5.0798 m (B is equal to the free surface length of the horizontal cylinder fluid), respectively. Excitation frequencies of 0.17, 0.47, and 0.77 rad/s are also considered for comparison.

Figure 3(a) indicates that the difference between the two force diagrams of a rectangular tank with a width of 2.1232 m and a horizontal cylindrical tank with a radius of 1.067 m is less than the difference between the two force diagrams of a rectangular tank with a width of 5.0798 m and a cylindrical tank with a radius of 3.84 m. Thus, it was observed that increasing the $\frac{h_0}{R}$ ratio resulted in a decrease in the difference between the force applied to the lateral wall of the horizontal cylindrical tank and the force applied to the lateral wall of the rectangular tank (with the same initial water depth and width equal to the length of water free surface in the horizontal cylindrical tank). This result can also be seen in the diagrams of Figs. 3(b) and 3(c), which are drawn at excitation frequencies farther from the frequency of the first mode of water sloshing in rectangular and horizontal cylindrical tanks. This indicates the accuracy of the relations and the solution process presented in Section 2.

To further investigate the difference between sloshing water inside horizontal cylindrical and rectangular tanks under the effect of longitudinal excitation, the time history diagram of the maximum height and force per unit width of water on the lateral wall was considered. The results reported by Chen et al. (2007) for a rectangular tank were compared with those of the equivalent horizontal cylindrical tank with equal initial depth and length. In addition, Chen et al.'s (2007) experimental study was compared with the same rectangular tank based on shallow water wave theory in order to investigate the accuracy of the numerical modeling done in this article. In the current study, in addition to harmonic excitation, two earthquake records of Chi-Chi (Taiwan 1999) and Kobe (Japan 1995) with a magnitude of 0.01 were utilized. The Chi-Chi earthquake record in this paper was taken from the east-west accelerogram of CHY028 station, and the Kobe earthquake record was taken from Port Island Station.

Chen et al. (2007) examined a rectangular tank with a length of 0.8 m, width of 0.141 m, initial water depth of 0.1 m, and a first mode water sloshing frequency of 3.79 rad/s under excitation along the tank length experimentally and using potential flow theory. For comparison, a horizontal cylindrical tank with the same initial depth and length of the rectangular tank with the minimum allowable radius of 0.12 m (according to section 2) was used in the present study. According to Eq. (16), the frequencies of the first mode of water sloshing inside

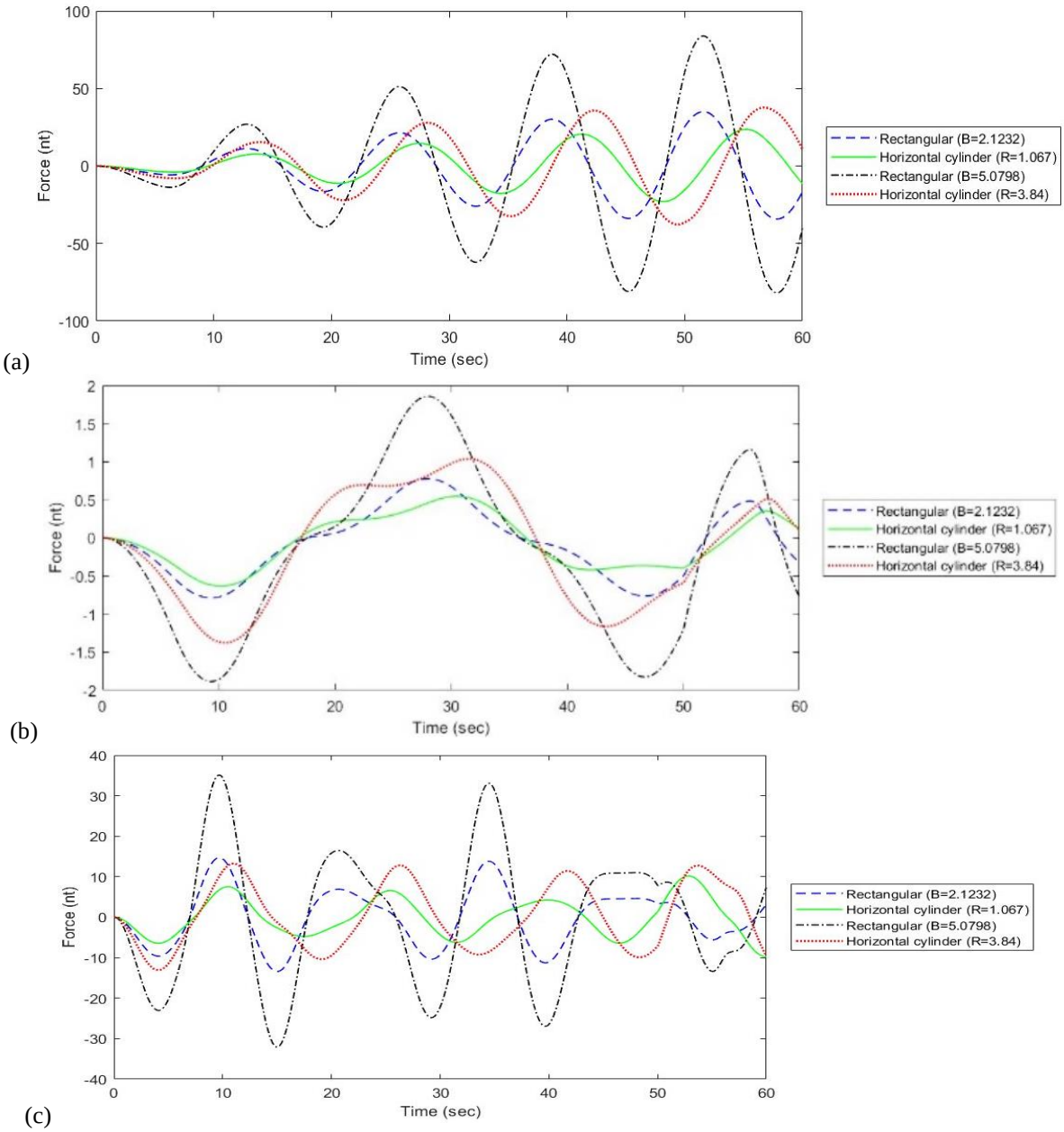

Fig. 3 Forces on the lateral wall of horizontal cylindrical and rectangular tanks, subjected to harmonic excitations of (a) 0.47 rad/s, (b) 0.17 rad/s and (c) 0.77 rad/s (nt=newton)

horizontal cylindrical tanks with radius of 0.12 m and 0.4 m were equal to 3.37 rad/s and 3.22 rad/s, respectively. The mesh size was considered to be n = 30.

As shown in Fig. 4(a), because the excitation frequency is close to the sloshing frequency of the water inside the horizontal cylindrical tank, a resonance phenomenon occurs, and over time, the maximum water height on the lateral wall of the horizontal cylindrical tank increases to more than that of the rectangular tank. In the rectangular tank, however, because its frequency is far from the excitation frequency, the water level on the lateral wall of the tank is damped and reduced over time. Conversely, in Fig. 4(b), the excitation frequency was exactly equal to the sloshing frequency of the water inside the rectangular tank, so as resonance occurred and over time, the water height on the lateral wall of the rectangular tank increased to more than that of the horizontal cylindrical tank. Fig. 4(c) indicates that under Kobe seismic excitation, the water height on the lateral wall of the rectangular tank was higher than that of the horizontal cylindrical tank, but in Fig. 4(d) and under the Chi-Chi seismic excitation, the maximum water height on the lateral wall of the horizontal cylindrical tank was higher in most parts of the graph. The results obtained from Figs. 4(a) to 4(d) show that the difference between the maximum height of water on the lateral wall of the horizontal cylindrical tank compared to the rectangular tank with the same length and initial depth of water depends on the excitation frequency. In some cases, therefore, the maximum water height can be higher than that of the rectangular tank, which can lead to greater force on the lateral wall of the horizontal cylindrical tank than that of the rectangular tank. Additionally, in all four diagrams of Fig. 4, the water elevation diagram on the lateral wall of the rectangular tank using the shallow liquid wave theory has an acceptable similarity

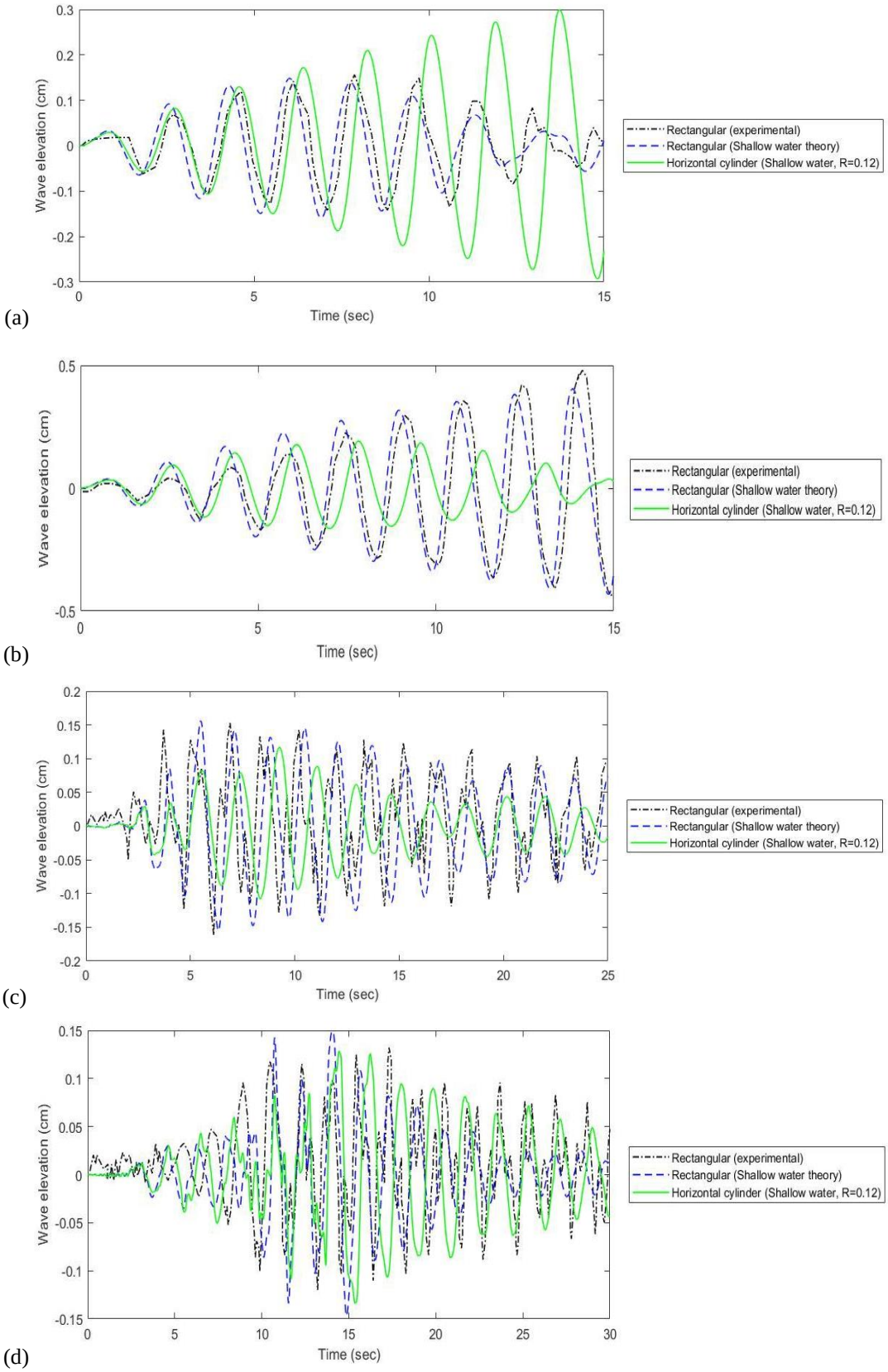

Fig. 4 Wave elevations on the lateral wall of rectangle and horizontal cylindrical tanks, subjected to harmonic excitations of (a) 3.41 rad/s and (b) 3.79 rad/s, and seismic excitations of (c) 1% kobe and (d) 1% Chi-Chi earthquakes

with the experimental results achieved by Chen et al. (2007). Therefore, it can be said that the numerical modeling of this study is sufficiently accurate, and the numerical verification performed in Fig. 3 for both the rectangular and horizontal cylindrical tanks is reliable.

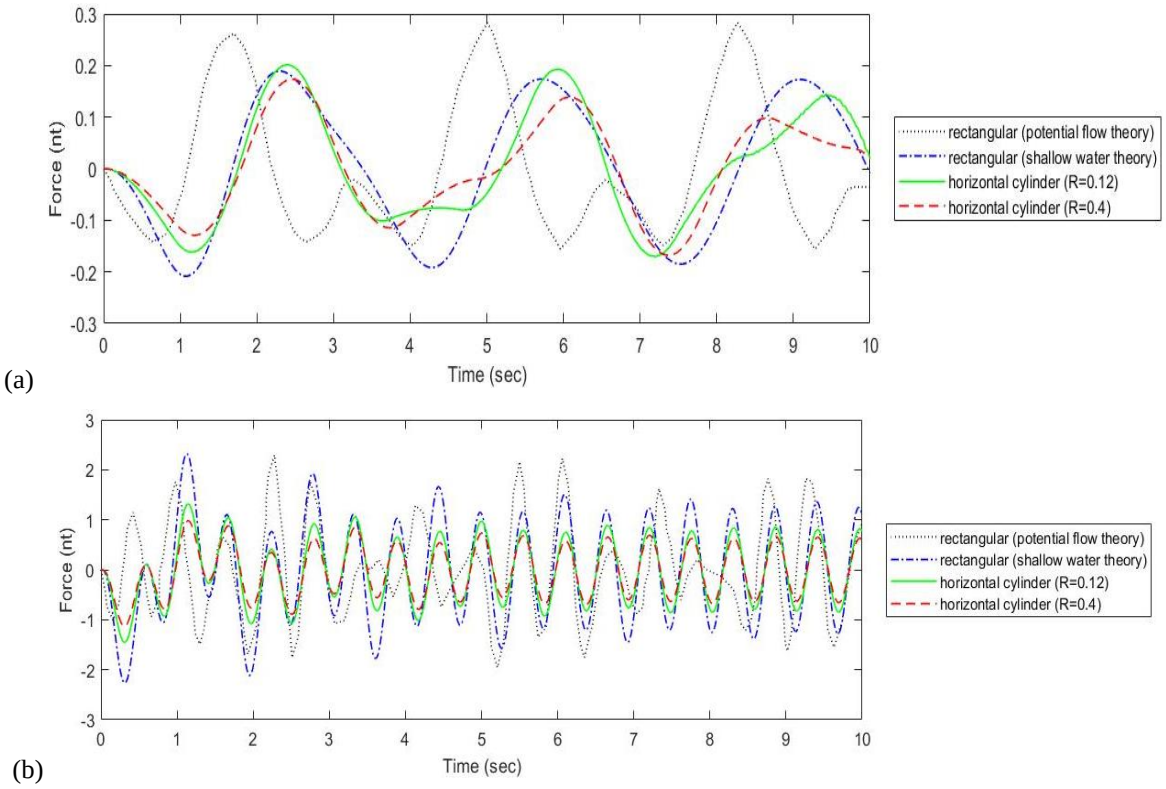

Fig. 5 Forces per unit width applied to the lateral wall of horizontal cylindrical and rectangular tanks, subjected to harmonic excitations of (a) 1.9 rad/s and (b) 11.38 rad/s

In Fig. 5, time history diagrams of force per unit width due to hydrostatic pressure applied to the lateral wall of horizontal cylindrical tanks were plotted using Shallow liquid wave theory under harmonic excitations of 1.9 rad/s and 11.38 rad/s, and compared with the time history diagrams of force per unit width applied to the lateral wall of the rectangular tanks, using Shallow liquid wave theory and potential flow (Chen et al., 2007). The reason for using force per unit width in these two diagrams was to reach a better comparison between the force applied to the lateral wall of horizontal and rectangular cylindrical tank. Thus, the force obtained on the lateral wall of each tank at a given moment is divided by the width of the free surface of water on the tank's lateral wall at that moment.

As shown in Fig. 5(a), under the 1.9 rad/s harmonic excitation, the force per unit width on the lateral wall of the horizontal cylindrical tank with a radius of 0.12 m using the shallow liquid wave theory is slightly greater than the force per unit width on the lateral wall of the rectangular tank using the shallow liquid wave theory at some points. However, in Fig. 5(b) and under the harmonic excitation of 11.38 rad/s, the force per unit width on the lateral wall of the rectangular tank is greater than the force per unit width on the lateral wall of the horizontal cylindrical tank. In addition, both diagrams of Fig. 5 show that increasing the radius of the horizontal cylindrical tank from 0.12 m to 0.4 m did not increase the force applied to the lateral wall of the tank and even reduced it in some cases. According to Fig. 5, it can be inferred that a greater or lesser force per unit width due to the hydrostatic pressure of the water on the lateral wall of the horizontal cylindrical tank relative to the rectangular tank with similar length and water depth depends on the excitation frequency.

3.3. Comparison of Required Length and Volume of Water

To compare the required length and volume of water between the two studied types of tank with equal water sloshing frequency and performance, two horizontal cylindrical tanks and several rectangular tanks with the same water sloshing frequency of 1 rad/s and 2 rad/s at different excitation frequencies were designed and compared for the three $\frac{h_0}{L_c}$ (or $\frac{h_0}{L_{re}}$) ratios of 0.15, 0.1, and 0.05. According to Eq. (23), the width of the rectangular tank did not interfere with the frequency of water sloshing along the length of the tank and was only effective in determining the force created on the lateral wall of the tank. Therefore, attempts were made to determine the width of the rectangular tank at each excitation frequency such that the performance of the two types of tank is almost the same in terms of the amount of force produced by the impact of water on their lateral walls. In Table 2, the characteristics of horizontal rectangular and cylindrical tanks designed for different $\frac{h_0}{L_c}$ (or $\frac{h_0}{L_{re}}$) ratios are given for two water sloshing frequencies of 1 and 2 rad/s. Horizontal cylindrical tanks are also designed for the minimum permitted ratios $\frac{h_0}{R}$ (according to Table 1). For numerical simulation, mesh size n = 50 was applied.

Table 2 Characteristics of horizontal tanks

$\omega_c = \omega_R = \omega_{\text{excited}} = 1$ rad/s		
$\frac{h_0}{L_c}\left(or\ \frac{h_0}{L_{re}}\right),\ \frac{h_0}{R}$	rectangular tank (m)	horizontal cylindrical tank (m)
$\frac{h_0}{L_c}=\frac{h_0}{L_{re}}=0.15,\ \frac{h_0}{R}=0.75$	L_{re}=13.52, h_0=2.028, B=1.92	L_c=10.75, h_0=1.61, R=2.15
$\frac{h_0}{L_c}=\frac{h_0}{L_{re}}=0.10,\ \frac{h_0}{R}=0.50$	L_{re}=9.366, h_0=0.94, B=0.9	L_c=6.86, h_0=0.686, R=1.372
$\frac{h_0}{L_c}=\frac{h_0}{L_{re}}=0.05,\ \frac{h_0}{R}=0.25$	L_{re}=4.77, h_0=0.24, B=0.28	L_c=3.32, h_0=0.166, R=0.664
$\omega_c = \omega_R = \omega_{\text{excited}} = 2$ rad/s		
$\frac{h_0}{L_c}\ (or\ \frac{h_0}{L_{re}}),\ \frac{h_0}{R}$	rectangular tank (m)	horizontal cylindrical tank (m)
$\frac{h_0}{L_c}=\frac{h_0}{L_{re}}=0.15,\ \frac{h_0}{R}=0.75$	L_{re}=3.38, h_0=0.507, B=0.49	L_c=2.69, h_0=0.4, R=0.537
$\frac{h_0}{L_c}=\frac{h_0}{L_{re}}=0.10,\ \frac{h_0}{R}=0.50$	L_{re}=2.342, h_0=0.234, B=0.22	L_c=1.71, h_0=0.171, R=0.343
$\frac{h_0}{L_c}=\frac{h_0}{L_{re}}=0.05,\ \frac{h_0}{R}=0.25$	L_{re}=1.2, h_0=0.06, B=0.061	L_c=0.829, h_0=0.041, R=0.166

It should be noted that the characteristics of the tanks in Table 2 are the same for other excitation frequencies except the width of the rectangular tank (B). In this study, frequency ratios (ratio of excitation frequency to sloshing frequency of water in the tank, $\varphi=\frac{\omega_{\text{excited}}}{\omega_{tank}}$) of 0.25, 0.5, 0.75, 1, 1.5, 2, 3 and 4, have been used.

For example, in Fig. 6, the approximate matching of the time histories of the force applied to the lateral wall of rectangular and horizontal cylindrical tanks designed for the $\frac{h_0}{L_c}\left(or\ \frac{h_0}{L_{re}}\right)=0.15$ ratio, is shown for the water sloshing frequencies of 1 rad/s, at all desired excitation frequencies.

According to the functional agreement shown in Fig. 6 between horizontal rectangular and cylindrical tanks with the same water sloshing frequency, the characteristics of the tanks designed in Table 2 show that when a cylindrical tank instead of a rectangular tank is used, a shorter tank length is required to produce the same value of lateral force. This is up to 20.5% for $\frac{h_0}{L_c}\left(or\ \frac{h_0}{L_{re}}\right)=0.15$, up to 27% for $\frac{h_0}{L_c}\left(or\ \frac{h_0}{L_{re}}\right)=0.10$, and up to 31% for $\frac{h_0}{L_c}\left(or\ \frac{h_0}{L_{re}}\right)=0.05$. Fig. 7 shows a graph of the changes in the volume ratio of water required by the horizontal cylindrical tank (V_{cy}) to the volume of water required by the rectangular tank (V_{re}) for the water sloshing frequencies of 1 rad/s and 2 rad/s to produce approximately the same force on the lateral walls of the two tanks for different frequencies and different ratios of $\frac{h_0}{L_c}\left(or\ \frac{h_0}{L_{re}}\right)$.

Examination of the diagrams in Fig. 7 reveals that in most cases, similar volumes of water are required for the horizontal rectangular and cylindrical tanks with the same sloshing frequency in order for them to perform similarly. In some instances, even the volume of water required for a horizontal cylindrical tank is slightly lower than that required for a rectangular tank. The results obtained from studying the diagrams of Figs. 5 to 7 indicate that for practical uses of the force produced by the sloshing of water inside the tank, for cases with architectural limitations in terms of length, using horizontal cylindrical tanks instead of rectangular tanks is a practical and useful solution.

3.4. The Effect of Fluid Viscosity

To compare the time history diagrams of the force applied to the lateral wall of the horizontal cylindrical tank by different fluids, two horizontal cylindrical tanks with ratios of $\frac{h_0}{L_c}=0.075$ and $\frac{h_0}{L_c}=0.15$ were used with dimensions and sloshing frequencies of the first fluid mode given in Table 3. The characteristics of the different fluids used in the horizontal cylindrical tank, including the values of dynamic viscosity and density, are shown in Table 4. The mesh size was considered to be n = 50.

Table 3 The characteristics of horizontal cylindrical tanks

case	$\frac{h_0}{L_c},\ \frac{h_0}{R}$	Characteristics (m)
1	$\frac{h_0}{L_c}=0.075,\ \frac{h_0}{R}=0.375\ (\frac{L_c}{R}=5)$	L_c=1.33, h_0=0.1, R=0.266, ω_c = 1.95 rad/s
2	$\frac{h_0}{L_c}=0.150,\ \frac{h_0}{R}=0.750\ (\frac{L_c}{R}=5)$	L_c=2.69, h_0=0.4, R=0.537, ω_c = 2 rad/s

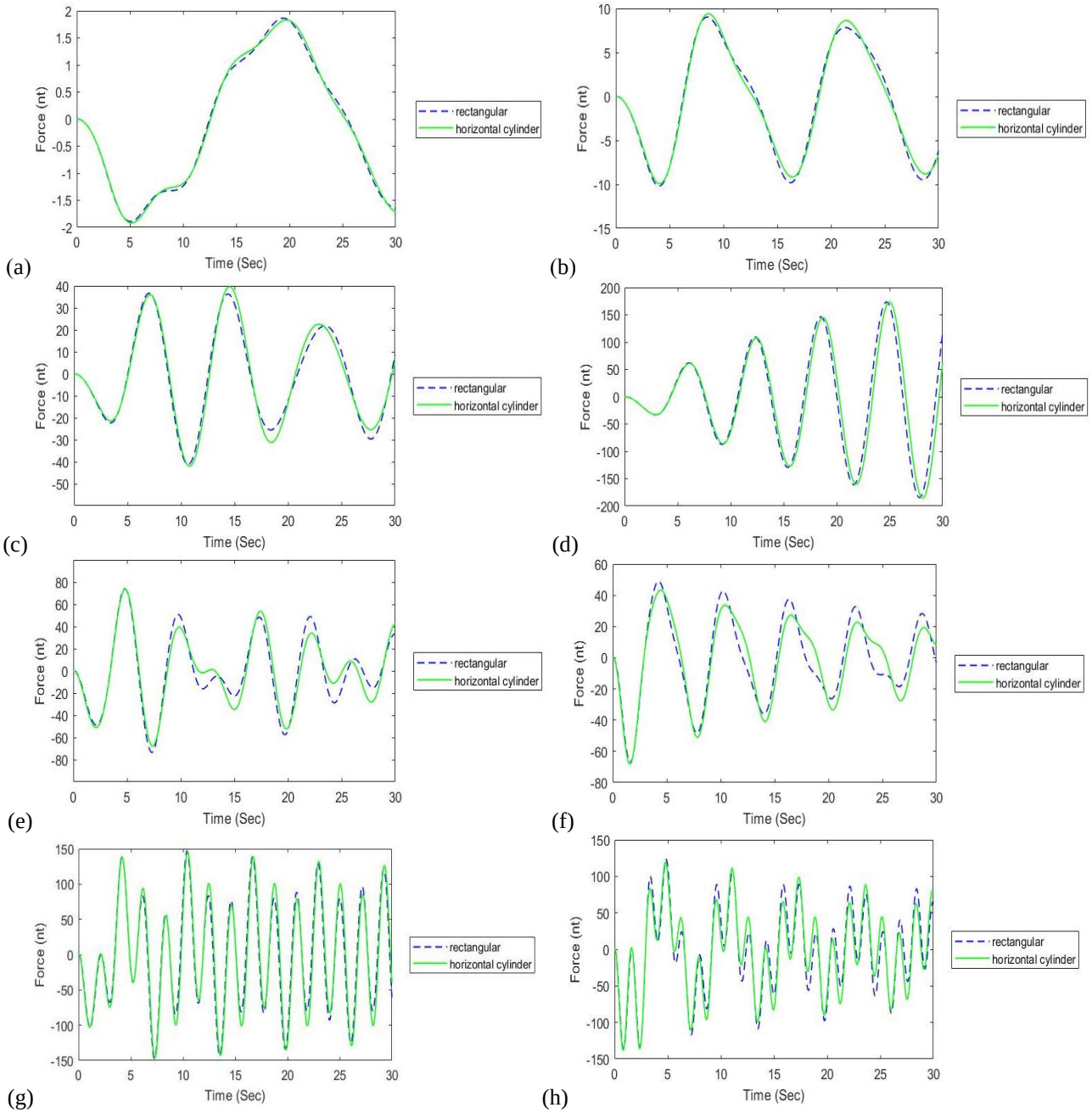

Fig. 6 Forces applied to the lateral walls of the rectangular and horizontal cylindrical tanks with the same water sloshing frequency of 1 rad/s and $\frac{h_0}{L_c}$ $(or$ $\frac{h_0}{L_{re}})$ $= 0.15$, subjected to frequency ratios of (a) $\varphi = 0.25$, (b) $\varphi = 0.5$, (c) $\varphi = 0.75$, (d) $\varphi = 1$, (e) $\varphi = 1.5$, (f) $\varphi = 2$, (g) $\varphi = 3$, (h) $\varphi = 4$.

Table 4 The characteristics of fluids

fluid	$\rho\ (\frac{kg}{m^3})$	$\mu\ (pa.s)$
20 °C water	1000	1.002×10^{-3}
ideal fluid	1000	0
40 °C water	992	0.653×10^{-3}
0 °C water	1000	1.787×10^{-3}
SAE 20w-20 oil	885	0.177
antifreeze (ethylene glycol)	1112	0.020016

In Figs. 8(a) and 8(b), the time history diagrams of the forces applied to the lateral wall of the case 1, using 20 °C water, 0 °C water, 40 °C water and the ideal fluid, are plotted under the harmonic excitation of 2 rad/s and the Kobe earthquake with a magnitude of 0.01.

As shown in Figs. 8(a) and 8(b), despite the difference between the viscosities of water at different temperatures, there was not much difference in the amount of force applied to the lateral wall of the tank. In fact, this result indicates that the difference in water viscosity at different temperatures is not high enough to make a significant difference in the amount of force applied to the lateral wall of the tank. However, as expected, when the dynamic viscosity was decreased, the force from the ideal fluid was slightly greater than 40 °C water, itself being slightly more than that of 20 °C water, which is slightly more than that of 0 °C water.

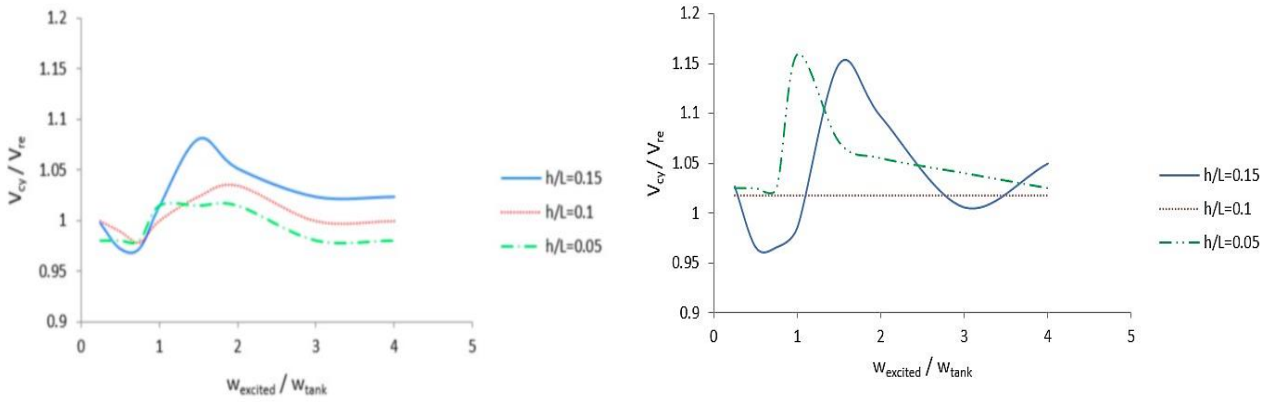

(a) (b)

Fig. 7 Changes in the volume ratio of water required by the horizontal cylindrical tank (V_{cy}) to the volume of water required by the rectangular tank (V_{re}) with the same performance, for the water sloshing frequency of (a) 1 rad/s and (b) 2 rad/s

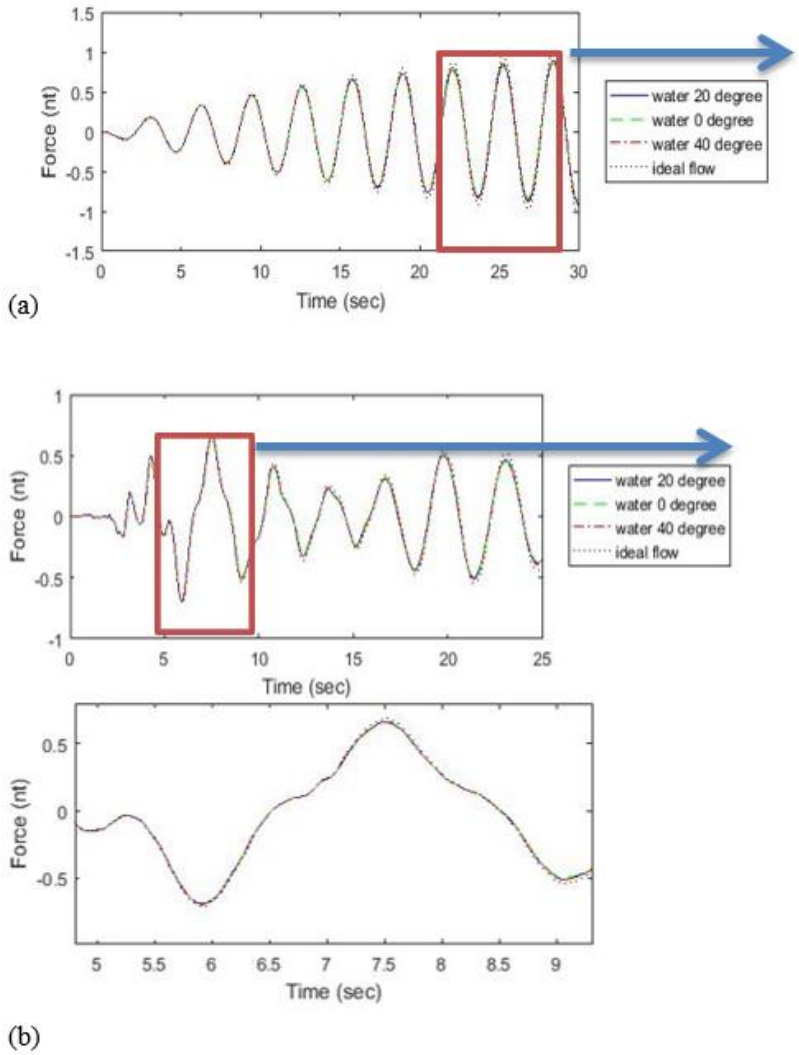

Fig. 8 Forces applied to the lateral wall of the case 1, using 20 °C water, 0 °C water, 40 °C water and the ideal fluid, subjected to (a) harmonic excitations of 2 rad/s and (b) seismic excitations of 1% kobe earthquake

In Fig. 9, the time history diagrams of the forces applied to the lateral wall of case 1 by 20 °C water, SAE 20w-20 oil, antifreeze (ethylene glycol), and the ideal fluid are shown under the harmonic excitation of 2 rad/s and the Kobe earthquake with an intensity of 0.01.

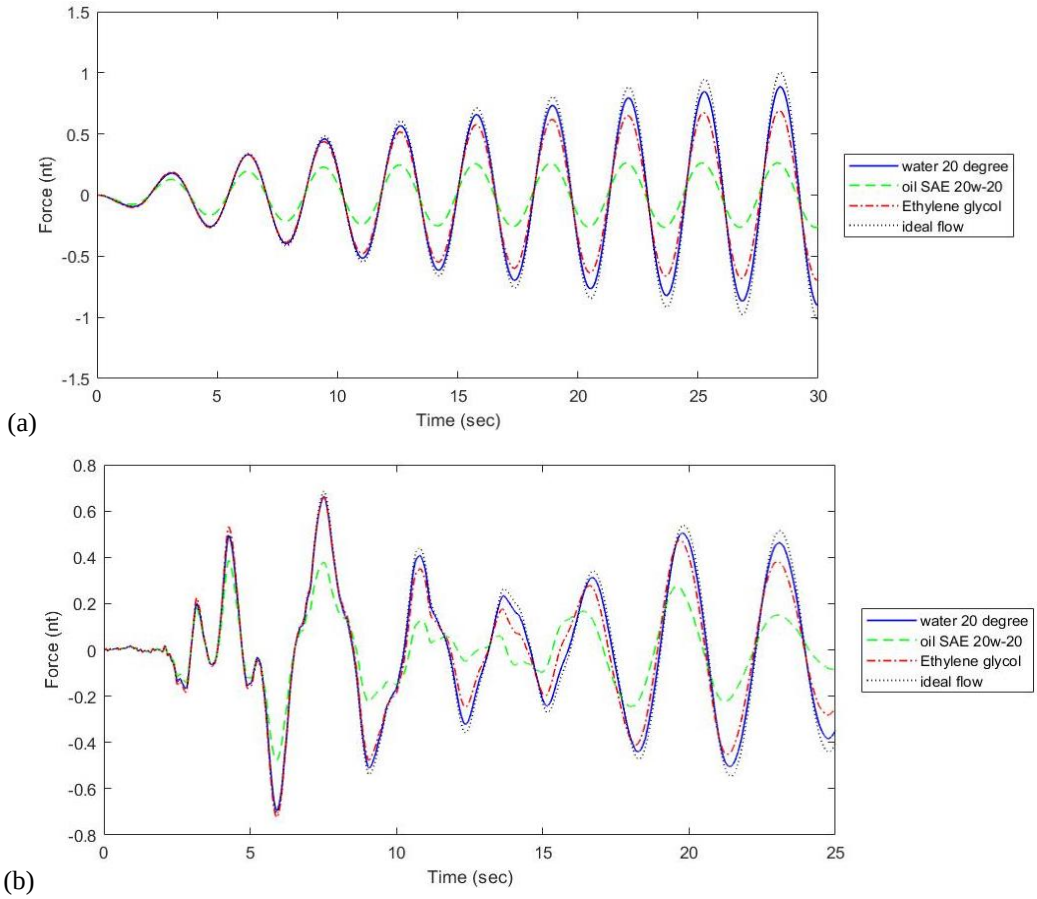

Fig. 9 Forces applied to the lateral wall of the cas 1, by 20 °C water, SAE 20w-20 oil, antifreeze (ethylene glycol) and the ideal flow, subjected to (a) harmonic excitations of 2 rad/s and (b) seismic excitations of 1% kobe earthquake

Figs. 9(a) and 9(b) show more clearly than Figs. 8(a) and 8(b) that the increase in dynamic viscosity causes a decrease in the force applied to the lateral wall of the horizontal cylindrical tank. As a result, the force applied to the lateral wall of the tank because of the ideal fluid was more than 20 °C degrees water, 20 °C water being more than antifreeze, and antifreeze being more than oil. However, as the antifreeze density was higher than water, it could be observed that this increase in antifreeze density compensates for the effect of increasing its viscosity by reducing the force applied to the lateral wall of the tank (relative to water). As a result, there is not much difference between the force applied to the lateral wall of the tank by water and that by antifreeze, and even at the peak of the Kobe earthquake (between 6 and 7 seconds in Fig. 9(b)), the two forces were almost equal. The same studies were performed in Figs. 10 and 11as in Figs. 8 and 9, respectively, this time for case 2 (with increased $\frac{h_0}{L_c}$ ratio compared to case 1).

Comparing the diagrams of Fig. 10 with those of Fig. 8 revealed that by increasing the $\frac{h_0}{L_c}$ ratio in case 2, the effect of fluid viscosity decreased and the graphs of water-induced force at different temperatures became closer to the graph of force due to the ideal flow.

The diagrams in Fig. 11 also show that by increasing the $\frac{h_0}{L_c}$ ratio in case 2, the effect of fluid viscosity on the diagram of the force applied to the lateral wall of the tank due to SAE 20w-20 antifreeze and oil relative to the ideal flow and 20 °C water was less than the diagrams in Fig. 9, such that the antifreeze force diagram is approximately equal to the 20 °C water force diagram and the ideal flow, and even at the peak of the Kobe earthquake, the antifreeze applied more force to the lateral wall of the horizontal cylindrical tank than the ideal flow and 20 °C water. This is also due to the higher density of antifreeze than water (and reduced viscosity effect).

4. SUMMARY AND CONCLUSIONS

In this study, a numerical model based on the shallow liquid wave theory was used to study the sloshing behaviors of a horizontal cylindrical tank under longitudinal harmonic and seismic excitation. The Navier–Stokes equations were solved in the longitudinal direction of the tank to account for the effect of shear stress of the tank bottom on fluid sloshing. Because the study considered the longitudinal direction of the tank, the validation of this numerical approach on the horizontal cylindrical tank was performed by bringing the cross-

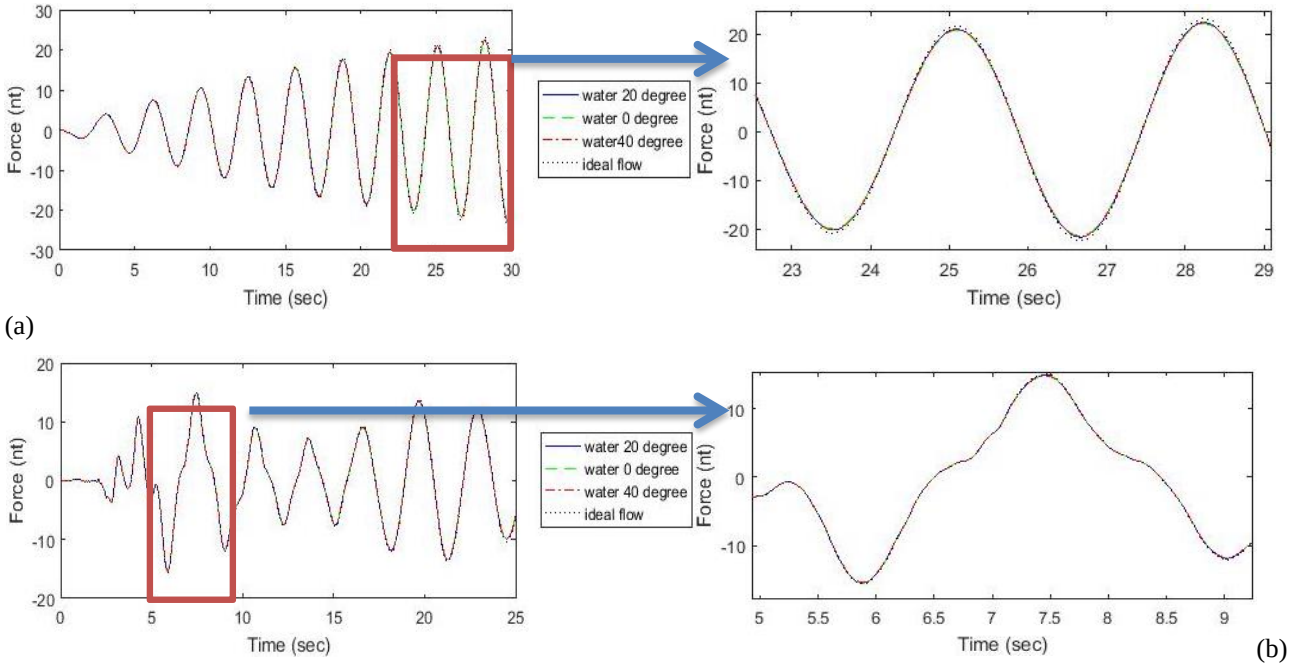

Fig. 10 Forces applied to the lateral wall of the case 2, using 20 °C water, 0 °C water, 40 °C water and the ideal fluid, subjected to (a) harmonic excitations of 2 rad/s and (b) seismic excitations of 1% kobe earthquake

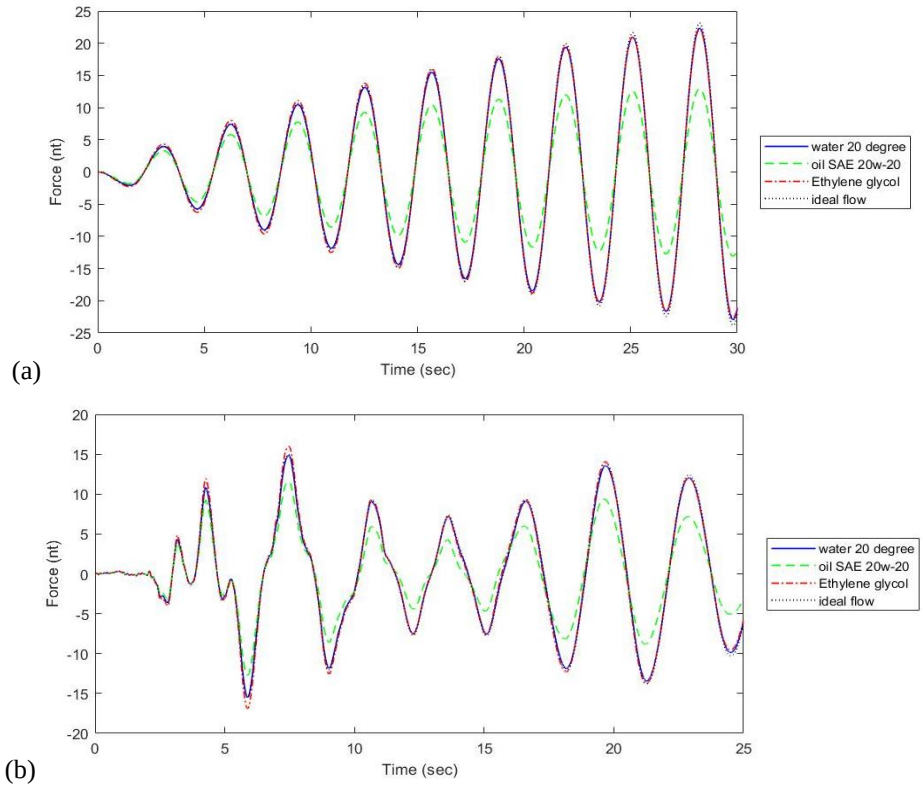

Fig. 11 Forces applied to the lateral wall of the cas 2, by 20 °C water, SAE 20w-20 oil, antifreeze (ethylene glycol) and the ideal flow, subjected to (a) harmonic excitations of 2 rad/s and (b) seismic excitations of 1% kobe earthquake.

sectional area of the fluid-filled section closer to the rectangular cross-section and comparing the results with previous numerical and experimental studies of the rectangular tank. The results indicate that the proposed method is reliable. The three important conclusions of this paper are: (1) The ability to make more use of the force applied to the lateral wall of the tank, between two horizontal cylindrical and rectangular tanks with the same

initial depth and length depends on the excitation frequency and can, in some cases, be higher in the horizontal cylindrical tank than in the rectangular tank (i.e., the excitation frequency being in phase with the sloshing frequency of the horizontal cylindrical tank fluid); (2) For practical use of the force applied to the lateral wall of the tank by the fluid in engineering purposes, when the designed rectangular tank has a longitudinal limit for on-site installation, the horizontal cylindrical tank can be used at the same excitation frequency as an alternative with almost the same volume of water but 26% less length on average; 3) Investigation of the effects of different fluids on the force applied to the lateral wall of the horizontal cylindrical tank showed that increasing the water temperature increased this force by a very small amount. Moreover, the increase in density causes an increase in the force, and it can reduce the effect of increasing the viscosity on reducing the force. In addition, increasing the ratio of the initial depth of the fluid to the length of the tank reduced the viscosity effect on this force. Finally, 20 °C water produced more force on the lateral wall of the tank than either antifreeze (Ethylene glycol) or SAE 20w-20 oil due to lower viscosity.

CONFLICTS OF INTEREST

The author(s) declared no potential conflicts of interest with respect to the research, authorship, and/or publication of this article.

AUTHORS CONTRIBUTION

A. H. Daneshmand: Methodology, Investigation, Data curation, Writing - Original draft preparation, Validation. **A. Karamodin:** Supervision, Project administration, Reviewing and Editing. **M. Pasandideh Fard:** Conceptualization, Supervision, Reviewing and Editing.

REFERENCES

Bhuta, P. G., & Koval, L. R. (1966). A viscous ring damper for a freely precessing satellite. *International Journal of Mechanical Sciences*, *8*, 383-395. https://doi.org/10.1016/0020-7403(66)90009-9

Carrier, G., & Miles, J. (1960). On the annular damper for a freely precessing gyroscope. *Journal of Applied Mechanics*, 237-240. https://doi.org/10.1115/1.3643944

Chen, B. F., & Chiang, H. W. (2000). Complete two-dimensional analysis of sea-wave-induced fully non-linear sloshing fluid in a rigid floating tank. *Ocean Engineering*, *27*, 953-977. https://doi.org/10.1016/S0029-8018(99)00036-0

Chen, W., Haroun, M. A., & Liu, F. (1996). Large amplitude liquid sloshing in seismically excited tanks. *Earthquake Engineering and Structural Dynamics*, *25*, 653-669. https://doi.org/10.1002/(SICI)1096-9845(199607)25:7<653::AID-EQE513>3.0.CO;2-H

Chen, Y. H., Hwang, W. S., & Ko, C. H. (2007). Sloshing behaviours of rectangular and cylindrical liquid tanks subjected to harmonic and seismic excitations. *Earthquake Engineering and Structural Dynamics*, *36*, 1701-1717. https://doi.org/10.1002/eqe.713

Dai, L., & Xu, L. (2006). A numerical scheme for dynamic liquid sloshing in horizontal cylindrical containers. *Proceedings of the Institution of Mechanical Engineers, Part D: Journal of Automobile Engineering*, *220*, 901-918. https://doi.org/10.1243/09544070D16604

De St Venant, B. (1871). Theorie du mouvement non-permanent des eaux avec application aux crues des rivers et a l'introduntion des Marees dans leur lit. *Academic de Sci. Comptes Redus*, *73*, 148-154.

Evans, D., & Linton, C. (1993). Sloshing frequencies. *The Quarterly Journal of Mechanics and Applied Mathematics*, *46*, 71-87. https://doi.org/10.1093/qjmam/46.1.71

Faltinsen, O. M., & Timokha, A. N. (2009). *Sloshing in marine-and land-based applications*. Cambridge University Press

Frandsen, J. B. (2004). Sloshing motions in excited tanks. *Journal of computational physics*, *196*, 53-87. https://doi.org/10.1016/j.jcp.2003.10.031

Gao, R., Wang, P., Sun, X., & Yang, S. (2021). Isogeometric boundary element analysis of liquid nonlinear sloshing in two dimensional rectangular tanks. *Computer Methods in Applied Mechanics and Engineering*, *387*, 114135. https://doi.org/10.1016/j.cma.2021.114135

Gholamipoor, M., & Ghiasi, M. (2022). Numerical analysis of fully non-linear sloshing waves in an arbitrary shape tank by meshless method. *Engineering Analysis with Boundary Elements*, *144*, 366-379. https://doi.org/10.1016/j.enganabound.2022.08.025

Goudarzi, M. A., & Sabbagh-Yazdi, S. R. (2012). Investigation of nonlinear sloshing effects in seismically excited tanks. *Soil Dynamics and Earthquake Engineering*, 43, 355-365. https://doi.org/10.1016/j.soildyn.2012.08.001

Gurusamy, S., & Kumar, D. (2020). Experimental study on nonlinear sloshing frequency in shallow water tanks under the effects of excitation amplitude and dispersion parameter. *Ocean Engineering*, *213*, 107761. https://doi.org/10.1016/j.oceaneng.2020.107761

Gurusamy, S., & Kumar, D. (2021). *Experimental study on shallow water sloshing*. Advances in Structural Vibration. Springer. https://doi.org/10.1007/978-981-15-5862-7_46

Hejazi, F. S. A., & Mohammadi, M. K. (2019). Investigation on sloshing response of water rectangular tanks under horizontal and vertical near fault seismic excitations. *Soil Dynamics and*

Earthquake Engineering, *116*, 637-653. https://doi.org/10.1016/j.soildyn.2018.10.015

Henderson, F. (1966). *Open channel flow*. Macmillan, New York

Housner, G. W. (1963). The dynamic behavior of water tanks. *Bulletin of the seismological society of America*, *53*, 381-387. https://doi.org/10.1785/BSSA0530020381

Ibrahim, R. A. (2005). *Liquid sloshing dynamics: theory and applications*. Cambridge University Press

Karamanos, S. A., & Kouka, A. (2016). A refined analytical model for earthquake-induced sloshing in half–full deformable horizontal cylindrical liquid containers. *Soil Dynamics and Earthquake Engineering*, *85*, 191-201. https://doi.org/10.1016/j.soildyn.2016.03.004

Kobayashi, N Kobayashi., Mieda, T., Shibata, H., & Shinozaki, Y. (1989). A study of the liquid slosh response in horizontal cylindrical tanks. *Journal of Pressure Vessel Technology*, 32-38. https://doi.org/10.1115/1.3265637

Koh, C., Mahatma, S., & Wang, C. (1994). Theoretical and experimental studies on rectangular liquid dampers under arbitrary excitations. *Earthquake engineering and structural dynamics*, *23*, 17-31. https://doi.org/10.1002/eqe.4290230103

Lu, M., Popplewell, N., Shah, A., & Chan, J. (2004). Nutation damper undergoing a coupled motion. *Journal of Vibration and Control*, *10*, 1313-1334. https://doi.org/10.1177/1077546304042045

McIver, P., & McIver, M. (1993). Sloshing frequencies of longitudinal modes for a liquid contained in a trough. *Journal of Fluid Mechanics*, *252*, 525-541. https://doi.org/10.1017/S0022112093003866

Moiseev, N., & Petrov, A. (1966). The calculation of free oscillations of a liquid in a motionless container. *Advances in Applied Mechanics*, 91-154, Elsevier. https://doi.org/10.1016/S0065-2156(08)70007-3

Moslemi, M., Farzin, A., & Kianoush, M. (2019). Nonlinear sloshing response of liquid-filled rectangular concrete tanks under seismic excitation. *Engineering Structures*, *188*, 564-577. https://doi.org/10.1016/j.engstruct.2019.03.037

Pandit, A., & Biswal, K. (2020). Evaluation of dynamic characteristics of liquid sloshing in sloped bottom tanks. *International journal of dynamics and control*, *8*, 162-177. https://doi.org/10.1007/s40435-019-00527-8

Papaspyrou, S., Karamanos, S., & Valougeorgis, D. (2004). Response of half–full horizontal cylinders under transverse excitation. *Journal of Fluids and Structures*, *19*, 985-1003. https://doi.org/10.1016/j.jfluidstructs.2004.04.014

Patkas, L. A., & Karamanos, S. A. (2007). Variational solutions for externally induced sloshing in horizontal-cylindrical and spherical vessels. *Journal of Engineering Mechanics*, *133*, 641-655. https://doi.org/10.1061/(ASCE)0733-9399(2007)133:6(641)

Reeve, D., Chadwick, A., & Fleming, C. (2018). *Coastal engineering: processes, theory and design practice*. CRC Press.

Roy, S. S., & Biswal, K. C. (2023). Non-linear finite element analysis of seismically excited sloped wall tank. *Ocean Engineering*, *267*, 113212. https://doi.org/10.1016/j.oceaneng.2022.113212

Saghi, R., & Saghi, H. (2022). Numerical simulation of half-full cylindrical and bi-lobed storage tanks against the sloshing phenomenon. *Ocean Engineering*, *266*, 112896. https://doi.org/10.1016/j.oceaneng.2022.112896

Shimizu, T., & Hayama, S. (1987). Nonlinear responsed of sloshing based on the shallow water wave theory: vibration, control engineering, engineering for industry. *JSME international journal*, *30*, 806-813. https://doi.org/10.1299/jsme1987.30.806

Stoker, J. J. (2011). *Water waves: The mathematical theory with applications*. John Wiley and Sons

Timokha, A. N. (2007). *Note on natural frequencies of longitudinal liquid sloshing in horizontal cylindrical tanks.* Proceedings of the Institute of Mathematics of NASU, Kiev, Ukraine. https://www.researchgate.net/publication/266915060_Note_on_natural_frequencies_of_longitudinal_liquid_sloshing_in_horizontal_cylindrical_tanks

Virella, J. C., Prato, C. A., & Godoy, L. A. (2008). Linear and nonlinear 2D finite element analysis of sloshing modes and pressures in rectangular tanks subject to horizontal harmonic motions. *Journal of Sound and Vibration*, *312*, 442-460. https://doi.org/10.1016/j.jsv.2007.07.088

Wu, G., Taylor, R. E., & Greaves, D. (2001). The effect of viscosity on the transient free-surface waves in a two-dimensional tank. *Journal of Engineering Mathematics*, *40*, 77-90. https://doi.org/10.1023/A:1017558826258

Yan, S. U., Yuan, X. Y., & Liu, Z. Y. (2020). Numerical researches of three-dimensional nonlinear sloshing in shallow-water rectangular tank. *Applied Ocean Research*, *101*, 102256. https://doi.org/10.1016/j.apor.2020.102256

APPENDIX A

Extraction of Governing Equations

St-Venant equations have been used to derive the equations governing the liquid sloshing inside the horizontal cylindrical tank along the length (De St Venant, 1871):

$$\frac{\partial Q}{\partial x}+\frac{\partial A}{\partial t}=0 \tag{A.1}$$

$$\frac{1}{A}\frac{\partial Q}{\partial t}+\frac{1}{A}\frac{\partial}{\partial x}\left(\frac{Q^2}{A}\right)+g\frac{\partial h}{\partial x}-g\left(\theta_B-S\right)=0 \tag{A.2}$$

Eq. (A.1) refers to the mass continuity equation and Eq. (A.2) refers to the momentum continuity equation. In these equations, Q, A, and θ_B represent discharge, cross-sectional area, and bed slope, respectively. Given $Q = AV$, Eq. (A.1) can be rewritten as follows:

$$V\frac{\partial A}{\partial x}+A\frac{\partial V}{\partial x}+\frac{\partial A}{\partial t}=0 \tag{A.3}$$

According to Fig. 1, the cross-sectional area of the fluid in the horizontal cylindrical tank is as follows:

$$A=R^2\cos^{-1}\left(\frac{R-h}{R}\right)-\left(R-h\right)\sqrt{2Rh-h^2} \tag{A.4}$$

therefore:

$$\frac{\partial A}{\partial x}=\left(\frac{4Rh-2h^2}{\sqrt{2Rh-h^2}}\right)\frac{\partial h}{\partial x}\ ,\ \frac{\partial A}{\partial t}=\left(\frac{4Rh-2h^2}{\sqrt{2Rh-h^2}}\right)\frac{\partial h}{\partial t} \tag{A.5}$$

According to Eqs. (A.3) to (A.5), Eq. (A.1) for horizontal cylindrical tank is finally obtained as follows:

$$V\left(\frac{4Rh-2h^2}{\sqrt{2Rh-h^2}}\right)\frac{\partial h}{\partial x}+\left(R^2\cos^{-1}\left(\frac{R-h}{R}\right)-\left(R-h\right)\sqrt{2Rh-h^2}\right)\frac{\partial V}{\partial x}+\left(\frac{4Rh-2h^2}{\sqrt{2Rh-h^2}}\right)\frac{\partial h}{\partial t}=0 \tag{A.6}$$

Considering $Q = AV$ and $\frac{\partial A}{\partial t}=-\frac{\partial Q}{\partial x}$ in Eq. (A.1), the first term of Eq. (A.2) can be written as follows:

$$\frac{1}{A}\frac{\partial Q}{\partial t}=\frac{V}{A}\frac{\partial A}{\partial t}+\frac{\partial V}{\partial t}=-\frac{V}{A}\frac{\partial Q}{\partial x}+\frac{\partial V}{\partial t}=-\frac{V^2}{A}\frac{\partial A}{\partial x}-V\frac{\partial V}{\partial x}+\frac{\partial V}{\partial t} \tag{A.7}$$

Also, according to $Q = AV$, the second term of Eq. (A.2) is obtained as follows:

$$\frac{1}{A}\frac{\partial}{\partial x}\left(\frac{Q^2}{A}\right)=\frac{1}{A}\frac{\partial}{\partial x}\left(AV^2\right)=\frac{V^2}{A}\frac{\partial A}{\partial x}+2V\frac{\partial V}{\partial x} \tag{A.8}$$

Given the Eqs. (A.7) and (A.8), and since the cylindrical tank is horizontal herein ($\theta_B = 0$), by adding the tank acceleration term $\left(\frac{\partial^2 x_B}{\partial t^2}\right)$ (Shimizu & Hayama, 1987), Eq. (A.2) for the horizontal cylindrical tank is obtained finally as follows:

$$\frac{\partial V}{\partial t}+V\frac{\partial V}{\partial x}+g\frac{\partial h}{\partial x}+gS+\frac{\partial^2 x_B}{\partial t^2}=0 \tag{A.9}$$

In Eq. (A.9), S represents the slope of the energy grade lines, which is generally calculated from the following equation:

$$S=\frac{\tau}{\rho g\Re} \tag{A.10}$$

were $\Re$ indicates the hydraulic radius obtained by dividing the area (A) by the wetted perimeter of the tank section (p):

$$\Re=\frac{A}{p} \tag{A.11}$$

Referring to Fig. 1, the wetted perimeter of the horizontal cylindrical tank cross section can be calculated from the following equation:

$$p=2R\cos^{-1}\left(\frac{R-h}{R}\right) \tag{A.12}$$

According to Eqs. (A.10) to (A.12) and Eq. (A.4) for the cross-sectional area of the fluid in the horizontal cylindrical tank, finally the slope of the energy grade lines for the horizontal cylindrical tank is obtained as follows:

$$S=\frac{\tau}{\rho g\left(\frac{R}{2}-\frac{\left(R-h\right)L}{4R\cos^{-1}\left(\frac{R-h}{R}\right)}\right)} \tag{A.13}$$

where L represents the length of the free surface of the liquid in Fig. 1:

$$L=2\sqrt{2Rh-h^2} \tag{A.14}$$

Although in the above procedure, the governing equations were extracted for the fluid below the tank half, they remain valid if the fluid passes through the tank half.

APPENDIX B

Determination of Shear Stress Of Horizontal Cylindrical Tank Bottom

The shear stress in the horizontal cylindrical tank bottom can be calculated from the following equation:

$$\tau=\mu\left.\frac{\partial v_x}{\partial r}\right|_{r=R} \tag{B.1}$$

here μ represents the dynamic viscosity of the fluid. Navier – Stokes equations are used to calculate the term $\frac{\partial v_x}{\partial r}$.

According to Fig. 1, the general form of the Navier – Stokes equations in polar coordinates along the length of the tank (x) is as follows:

$$\left(\frac{\partial v_x}{\partial t}+v_r\frac{\partial v_x}{\partial r}+\frac{v_\theta}{r}\frac{\partial v_x}{\partial \theta}+v_x\frac{\partial v_x}{\partial x}\right)=-\frac{\partial p}{\partial x}+\rho g_x+\mu\left[\frac{1}{r}\frac{\partial}{\partial r}\left(r\frac{\partial v_x}{\partial r}\right)+\frac{1}{r^2}\frac{\partial^2 v_x}{\partial \theta^2}+\frac{\partial^2 v_x}{\partial x^2}\right] \tag{B.2}$$

Given that the parameters of velocity derivative with respect to length ($\frac{\partial v_x}{\partial x}$), velocity derivative with respect to angle ($\frac{\partial v_x}{\partial \theta}$), density changes ($\frac{\partial p}{\partial x}$), longitudinal acceleration of ground (g_x) and velocity components in

polar coordinates (v_r *and* v_θ) are zero along the length of the tank, and also $\mu = \rho\vartheta$, Eq. (B.2) is simplified as follows:

$$\vartheta\left[\frac{1}{r}\frac{\partial}{\partial r}\left(r\frac{\partial v_x}{\partial r}\right)\right]=\frac{\partial v_x}{\partial t} \tag{B.3}$$

Assuming the application of harmonic oscillation to the tank as $(v_x = v_0 e^{i\omega t})$, the fluid velocity near the bottom of the tank oscillates at the same frequency. Given this fact and the expansion of Eq. (B.3) we have:

$$\left[\frac{1}{r}\frac{\partial}{\partial r}\left(r\frac{\partial v_x}{\partial r}\right)\right]=\frac{i\omega}{\vartheta}v_x \rightarrow \frac{\partial^2 v_x}{\partial r^2}+\frac{1}{r}\frac{\partial v_x}{\partial r}-\frac{i\omega}{\vartheta}v_x=0 \tag{B.4}$$

Multiplying Eq. (B.4) by r^2 gives the modified Bessel of the second type equation as follows:

$$r^2\frac{d^2 v_x}{dr^2}+r\frac{dv_x}{dr}-\frac{i\omega}{\vartheta}r^2 v_x=0 \tag{B.5}$$

The general solution to Eq. (B.5) is as follows:

$$v_x = AI_0\left(\sqrt{i\frac{\omega}{\vartheta}}r\right)+BK_0\left(\sqrt{i\frac{\omega}{\vartheta}}r\right) \tag{B.6}$$

Since the Bessel functions I_0 and K_0 in Eq. (B.6) were obtained in terms of the imaginary value $\left(\sqrt{i\frac{\omega}{\vartheta}}r\right)$, to resolve the ambiguity by considering $X=\sqrt{\frac{\omega}{\vartheta}}r$, they are written in the following form of Kelvin functions:

$$I_0\left(Xi^{1/2}\right)=ber\left(X\right)+ibei\left(X\right),$$
$$K_0\left(Xi^{1/2}\right)=Ker\left(X\right)+iKei\left(X\right) \tag{B.7}$$

Finally, the Bessel Eq. (B.6) is solved as a combination of real and imaginary functions of Kelvin, by solving the issue of being imaginary:

$$v_x = A\left(ber\left(X\right)+ibei\left(X\right)\right)+B\left(\ker\left(X\right)+ikei\left(X\right)\right) \tag{B.8}$$

Given the zero velocity changes relative to the radius at the fluid surface (maximum fluid height point) and the fact that the velocity of the fluid is equal to the excitation velocity near the bottom of the tank, and also one-dimensionality of the study, the following boundary conditions are applied to determine the constant coefficients A and B in Eq. (B.8):

$$\begin{cases} if\ R>h: r=R-h\rightarrow \dfrac{\partial v_x}{\partial r}=0 \\ \qquad\qquad or \\ if\ R<h: r=h-R\rightarrow \dfrac{\partial v_x}{\partial r}=0 \end{cases} \tag{B.9}$$

and

$$r=R\rightarrow v_x = v_0 e^{i\omega t} \tag{B.10}$$

Boundary condition (B.9) was written in two parts to include both fluid at the above and below of the half tank. For ease of display, the following variables have been changed:

$$\begin{cases} if\ R>h\rightarrow \gamma=\sqrt{\dfrac{\omega}{\vartheta}}\left(R-h\right) \\ if\ R<h\rightarrow \gamma=\sqrt{\dfrac{\omega}{\vartheta}}\left(h-R\right) \end{cases} \tag{B.11}$$

and

$$\sqrt{\frac{\omega}{\vartheta}}R=\lambda \tag{B.12}$$

Because Kelvin functions are not defined for a value of zero, if $h = R$ occurs, the value of h can be replaced with a value of $h + 0.00001$ with some error.

By applying the boundary conditions (B.9) and (B.10) in Eq. (B.8) and determining the coefficients *A* and *B*, Eq. (B.8) is obtained as follows:

$$\begin{aligned} v_x = &(\left(\left(ber_1\gamma+bei_1\gamma+i\left(bei_1\gamma-ber_1\gamma\right)\right)\right.\\ &\left(ker\left(X\right)+ikei\left(X\right)\right)-(ber\left(X\right)\\ &+ibei\left(X\right))\left(ker_1\gamma+kei_1\gamma+i\left(kei_1\gamma-ker_1\gamma\right)\right))\\ &(-bei_1\gamma kei\,\lambda+bei_1\gamma ker\,\lambda+bei\,\lambda\, kei_1\gamma-bei\,\lambda ker_1\gamma\\ &+ber_1\gamma kei\,\lambda+ber_1\gamma ker\,\lambda-ber\,\lambda\, kei_1\gamma-ber\,\lambda\, ker_1\gamma\\ &-i\,(bei_1\gamma kei\,\lambda+bei_1\gamma ker\,\lambda-bei\,\lambda\, kei_1\gamma\\ &-bei\,\lambda\, ker_1\gamma+ber_1\gamma kei\,\lambda-ber_1\gamma ker\,\lambda\\ &-ber\,\lambda\, kei_1\gamma+ber\,\lambda\, ker_1\gamma)))\frac{v_0 e^{i\omega t}}{C_1} \end{aligned} \tag{B.13}$$

The coefficient C_1 can be calculated in Eq. (B.13) from the following equation:

$$\begin{aligned} C_1 = &2(bei_1\gamma)^2(kei\,\lambda)^2+2(bei_1\gamma)^2\left(ker\,\lambda\right)^2\\ &-4bei_1\gamma bei\,\lambda\, kei_1\gamma kei\,\lambda-4bei_1\gamma bei\,\lambda\, ker_1\gamma ker\,\lambda\\ &-4bei_1\gamma ber\,\lambda\, kei_1\gamma ker\,\lambda+4bei_1\gamma ber\,\lambda kei\,\lambda\, ker_1\gamma\\ &+2\left(bei\,\lambda\right)^2(kei_1\gamma)^2+2(bei\,\lambda)^2(ker_1\gamma)^2\\ &+4bei\,\lambda\, ber_1\gamma\, kei_1\gamma ker\,\lambda-4bei\,\lambda\, ber_1\gamma kei\,\lambda\, ker_1\gamma\\ &+2(ber_1\gamma)^2(kei\,\lambda)^2+2(ber_1\gamma)^2\left(ker\,\lambda\right)^2\\ &-4ber_1\gamma ber\,\lambda\, kei_1\gamma kei\,\lambda-4ber_1\gamma ber\,\lambda\, ker_1\gamma ker\,\lambda\\ &+2\left(ber\,\lambda\right)^2(kei_1\gamma)^2+2(ber\,\lambda)^2(ker_1\gamma)^2 \end{aligned} \tag{B.14}$$

In Eq. (B.13), we write the parameter $e^{i\omega t}$ as $cos(\omega t)+isin(\omega t)$ and expand the equation. Then, instead of the variable *X*, we substitute its initial value in terms of *r* (i.e., $\sqrt{\frac{\omega}{\vartheta}}r$) and derive from the real part of the

equation relative to r to achieve the shear stress relation of the horizontal cylindrical tank bottom as follows:

$$\tau = \mu \frac{\partial v_x}{\partial r}\bigg|_{r=R} = \tau = \sqrt{2}\frac{D}{C_1}\rho\sqrt{\omega\vartheta}v_0\cos\left(\omega t + \varphi\right) \qquad \text{(B.15)}$$

Note that the imaginary part of Eq. (B.13) is related to changes in the longitudinal velocity of the fluid in the direction of the tank height, and since in Shallow liquid wave theory , the velocity profile is considered uniform in the vertical direction, its derivative with respect to r was omitted. In Eq. (B.15), the variable *D* in the coordinates *r*=*R*, ($X = \sqrt{\frac{\omega}{\vartheta}}R$) is calculated from the following equation:

$$\begin{aligned}
D = &((((\left(\left(-kei\,\lambda - ker\,\lambda\right)kei_1\gamma + ker_1\gamma\left(kei\,\lambda - ker\,\lambda\right)\right)bei_1\gamma \\
&+((-kei\,\lambda + ker\,\lambda)kei_1\gamma - ker_1\gamma\left(kei\,\lambda + ker\,\lambda\right))ber_1\gamma \\
&+\left((kei_1\gamma)^2 + (ker_1\gamma)^2\right)(bei\,\lambda + ber\,\lambda))bei_1(X) \\
&+(\left(\left(kei\,\lambda - ker\,\lambda\right)kei_1\gamma + ker_1\gamma\left(kei\,\lambda + ker\,\lambda\right)\right)bei_1\gamma \\
&+\left(\left(-kei\,\lambda - ker\,\lambda\right)kei_1\gamma + ker_1\gamma\left(kei\,\lambda - ker\,\lambda\right)\right)ber_1\gamma - ((kei_1\gamma)^2 \\
&+(ker_1\gamma)^2)(bei\,\lambda - ber\,\lambda))ber_1(X) + ((kei\,\lambda + ker\,\lambda)\,(bei_1\gamma)^2 \\
&+((-bei\,\lambda - ber\,\lambda)kei_1\gamma - ker_1\gamma\left(bei\,\lambda - ber\,\lambda\right))bei_1\gamma \\
&+(\left(kei\,\lambda + ker\,\lambda\right)ber_1\gamma + (bei\,\lambda - ber\,\lambda)kei_1\gamma \\
&-ker_1\gamma\left(bei\,\lambda + ber\,\lambda\right))ber_1\gamma)kei_1(X) - ((kei\,\lambda - ker\,\lambda)\,(bei_1\gamma)^2 \\
&+\left(\left(-bei\,\lambda + ber\,\lambda\right)kei_1\gamma + ker_1\gamma\left(bei\,\lambda + ber\,\lambda\right)\right)bei_1\gamma \\
&+(\left(kei\,\lambda - ker\,\lambda\right)ber_1\gamma + \left(-bei\,\lambda - ber\,\lambda\right)kei_1\gamma \\
&-ker_1\gamma\left(bei\,\lambda - ber\,\lambda\right))ber_1\gamma)ker_1(X))^2 \\
&+((((-kei\,\lambda + ker\,\lambda)kei_1\gamma - ker_1\gamma\left(kei\,\lambda + ker\,\lambda\right))bei_1\gamma \\
&+(\left(kei\,\lambda + ker\,\lambda\right)kei_1\gamma - ker_1\gamma\left(kei\,\lambda - ker\,\lambda\right))ber_1\gamma \\
&+\left((kei_1\gamma)^2 + (ker_1\gamma)^2\right)(bei\,\lambda - ber\,\lambda))bei_1(X) \\
&+(\left(\left(-kei\,\lambda - ker\,\lambda\right)kei_1\gamma + ker_1\gamma\left(kei\,\lambda - ker\,\lambda\right)\right)bei_1\gamma \\
&+(\left(-kei\,\lambda + ker\,\lambda\right)kei_1\gamma - ker_1\gamma\left(kei\,\lambda + ker\,\lambda\right))ber_1\gamma \\
&+\left((kei_1\gamma)^2 + (ker_1\gamma)^2\right)(bei\,\lambda + ber\,\lambda))ber_1(X) + ((kei\,\lambda - ker\,\lambda)\,(bei_1\gamma)^2 \\
&+\left(\left(-bei\,\lambda + ber\,\lambda\right)kei_1\gamma + ker_1\gamma\left(bei\,\lambda + ber\,\lambda\right)\right)bei_1\gamma \\
&+(\left(kei\,\lambda - ker\,\lambda\right)ber_1\gamma + \left(-bei\,\lambda - ber\,\lambda\right)kei_1\gamma - ker_1\gamma(bei\,\lambda \\
&-ber\,\lambda))ber_1\gamma)kei_1(X) + ((kei\,\lambda + ker\,\lambda)\,(bei_1\gamma)^2 \\
&+((-bei\,\lambda - ber\,\lambda)kei_1\gamma - ker_1\gamma\left(bei\,\lambda - ber\,\lambda\right))bei_1\gamma \\
&+(\left(kei\,\lambda + ker\,\lambda\right)ber_1\gamma + \left(bei\,\lambda - ber\,\lambda\right)kei_1\gamma \\
&-ker_1\gamma\left(bei\,\lambda + ber\,\lambda\right))ber_1\gamma)ker_1(X))^2)^{0.5}
\end{aligned} \qquad \text{(B.16)}$$

Since Eq. (B.15) was obtained by assuming harmonic excitation, it is only suitable for harmonic excitation. Therefore, considering $\cos(\omega t + \varphi) = 1$ in Eq. (B.15) for reliability, the shear stress equation of horizontal cylindrical tank bottom, is obtained as follows under the effect of any kind of excitation:

$$\tau = \mu \frac{\partial v_x}{\partial r}\bigg|_{r=R} = \tau = \sqrt{2}\frac{D}{C_1}\rho\sqrt{\omega\vartheta}v_0 \qquad \text{(B.17)}$$